Title:

A minimal "push-pull" bistability model explains oscillations between quiescent and proliferative cell states.

Sandeep Krishna[a,1] and Sunil Laxman[b,1]

[a]Simons Centre for the study of Living Machines, National Centre for Biological Sciences, Tata Institute of Fundamental Research.

[b]Institute for Stem Cell Biology and Regenerative Medicine.

GKVK post, Bellary Road

Bangalore 560065

[1]Correspondence: sandeep@ncbs.res.in and sunil@instem.res.in

Abstract

A minimal model for oscillating between quiescent and growth/proliferation states, dependent on the availability of a central metabolic resource, is presented. From the yeast metabolic cycles (YMCs), metabolic oscillations in oxygen consumption are represented as transitions between quiescent and growth states. We consider metabolic resource availability, growth rates, and switching rates (between states) to model a relaxation oscillator explaining transitions between these states. This frustrated bistability model reveals a required communication between the metabolic resource that determines oscillations, and the quiescent and growth state cells. Cells in each state reflect memory, or hysteresis of their current state, and “push-pull” cells from the other state. Finally, a parsimonious argument is made for a specific central metabolite as the controller of switching between quiescence and growth states. We discuss how an oscillator built around the availability of such a metabolic resource is sufficient to generally regulate oscillations between growth and quiescence, through committed transitions.

Keywords: quiescence, growth, metabolic oscillation, bistability, acetyl-CoA, NADPH

Introduction

While all cells can exist in a variety of states, two opposite ends of the spectrum are the "growth" state (leading to mitotic division and proliferation), and a non-proliferative "quiescent" state. The quiescent state, operationally defined here as a reversibly non-dividing state, is the predominant state of all living cells (Lewis and Gattie, 1991; Gray *et al.*, 2004). Understanding how cells reversibly transition from a quiescent state, to a growth state coupled with cell division and proliferation (henceforth called "growth" in this manuscript) is therefore a fundamental biological question. Current explanations for how cells commit to growth and cell division account for metabolic regulation, biomolecule synthesis, and regulated progression through the cell cycle, presenting multiple, integrated mechanisms of information transfer within a cell that lead to the eventual growth outcome.

However, when a population of genetically identical cells are present in a uniform environment, how can individual cells within such a population decide to switch between a quiescent (effective "G0") state and a growth/proliferation state? Indeed, such heterogeneity of cell states within populations is widely observed and acknowledged. Numerous examples exist in nearly all systems studied, from simple eukaryotes like the budding yeast, to complex mammalian systems (Cooper, 1998, 2003; Coller *et al.*, 2006; Daignan-Fornier and Sagot, 2011; Klosinska *et al.*, 2011; De Virgilio, 2012; Dhawan and Laxman, 2015), with multiple molecular events correlating with transitions between growth and quiescence. For any population transitioning into either of these states, experimentalists have asked: (i) what hallmarks allow discrimination between actively proliferating and G0 cells? (ii) how do cells transit back and forth between these two states? And (iii) how are different signals processed and integrated into an appropriate cellular response? The regulation of the final cellular outcome occurs at multiple levels, including differential gene expression programs, and signaling responses to growth factors, which can be different depending upon the type of cell or organism studied. At its very core, however, this transition between quiescent and growth states is a metabolic problem; cells must be in a metabolic state capable of

63 committing to growth/proliferation, and must sense this state, which the pushes cells
64 towards growth. Indeed, several lines of evidence now reiterate a primary metabolic
65 determinant for cells committing to a growth state (exiting quiescence), or remaining in a
66 quiescent state (Futcher, 2006; Daignan-Fornier and Sagot, 2011; Laporte *et al.*, 2011;
67 Cai and Tu, 2012; De Virgilio, 2012; Lee and Finkel, 2013; Dhawan and Laxman, 2015;
68 Kalucka *et al.*, 2015; Kaplon *et al.*, 2015). While multiple factors can regulate the
69 transition between quiescence and growth, all such studies suggest that without this
70 core metabolic transformation, switching states is impossible. Given this absolute
71 metabolic requirement to switch to growth, if there is an isogenic ("identical") population
72 of cells present in a uniform environment, how can there be a two-state outcome where
73 some cells undergo growth/proliferation, while the rest remain quiescent?
74
75 Surprisingly, there are few rigorous theoretical, mathematical models that attempt to
76 provide a conceptual framework sufficient to explain this, and suggest experimentally
77 testable predictions. This is in contrast to the extensive, elegant, and often prescient
78 models that have been built to explain progress through the classical cell division cycle
79 (CDC), by incorporating existing experimental data of phase specific cell-cycle
80 activators and inhibitors (Tyson and Novak, 2001; Tyson *et al.*, 2003; Ferrell *et al.*,
81 2009; Tyson and Novák, 2015). Such modeling of the CDC has a long history
82 (examples include (Goldbeter, 1991; J, 1991; Norel and Agur, 1991; Novak and Tyson,
83 1993; Ferrell *et al.*, 2009; Tyson and Novák, 2015)), and these types of theoretical
84 studies have revealed biological possibilities that were experimentally determined only
85 much later (such as (Cross *et al.*, 2002; Pomerening *et al.*, 2003; Wei *et al.*, 2003;
86 Mirchenko and Uhlmann, 2010)). Given this, there is considerable value in building
87 coarse-grained but rigorous theoretical models to understand switching between
88 quiescence and growth states. In such a model, the switching between quiescence and
89 growth states could be treated as a biological oscillation (Tyson *et al.*, 2003; Novák and
90 Tyson, 2008; Tsai *et al.*, 2008; Ferrell *et al.*, 2009), while considering a dependence on
91 a metabolic "resource" as a driver of the oscillator. For building such a model, we
92 therefore require extensive experimental data from biological systems where metabolic
93 oscillations are demonstrably closely coupled with exiting quiescence/entering the CDC.

Such data are readily available from the budding yeast, S. cerevisiae. Yeast have been the instrumental cellular model in revealing processes that define both the CDC (Hartwell, 1974), and the quiescence cycle (Gray *et al.*, 2004; Daignan-Fornier and Sagot, 2011; Daignan-Fornier B and Sagot I, 2011; De Virgilio, 2012; Dhawan and Laxman, 2015). The classical CDC involves progression through the G1, S, and G2/M phases. In contrast, during a quiescence (or effective “G0”) cycle, cells remain non-dividing, but can exit quiescence and enter the G1 phase of the cell cycle to subsequently complete the CDC.

Experimentally dissecting specific processes driving entry into, and exit from, quiescence (into the CDC) is challenging in asynchronous, heterogeneous cultures of cells. However, synchronized yeast populations in well-mixed cultures (as manifest by oscillations in oxygen consumption) have long been observed and studied using batch and chemostat conditions limited for a carbon source (glucose or ethanol), which are subsequently fed continuously with limited concentrations of glucose or ethanol (Chance *et al.*, 1964; Hommes, 1964; Hess and Boiteux, 1971; Satroutdinov *et al.*, 1992; Keulers *et al.*, 1996; Jules *et al.*, 2005; Lloyd and Murray, 2005). Gene expression studies from such glucose-limited yeast metabolic cycles or oscillations (we will utilize the term YMC henceforth in this manuscript for consistency) showed that a majority of the genome is expressed highly periodically, further revealing a molecular organization of growth and quiescent states (Klevecz *et al.*, 2004; Tu *et al.*, 2005; Futcher, 2006; Mellor, 2016). In general, both the shorter (Klevecz *et al.*, 2004; Murray *et al.*, 2007), and the longer oxygen consumption oscillations in yeast (Tu *et al.*, 2005) showed this general pattern. Notably, genes associated with biosynthesis and growth (comprehensively further described in (Brauer *et al.*, 2008)) typically peak during a high oxygen consumption phase in the YMC (Tu *et al.*, 2005; Rowicka *et al.*, 2007; Slavov and Botstein, 2011, 2013), while genes that mark autophagy, vacuolar function and a “quiescence” state peak during a steady, low oxygen consumption phase. Strikingly, in these continuous YMC cultures, cell division is tightly gated to a temporal window. Cells divide synchronously only once during each metabolic cycle (Küenzi and Fiechter, 1969; Tu *et al.*, 2005; Robertson *et al.*, 2008; Laxman *et al.*, 2010) and remain in a non-

125 dividing state during the rest of the cycle. The non-dividing population in the low oxygen
126 consumption phase exhibits typical hallmarks of quiescent cells (Tu *et al.*, 2005, 2007;
127 Shi *et al.*, 2010; Cai *et al.*, 2011; Shi and Tu, 2013; Dhawan and Laxman, 2015).
128 Furthermore, in each YMC, during the tight temporal window when cells do divide, the
129 culture has two, visibly distinct sub-populations: dividing and nondividing (Tu *et al.*,
130 2005; Robertson *et al.*, 2008; Laxman *et al.*, 2010). These data have suggested a close
131 coupling between the metabolic and the cell division cycles. Importantly, the YMC itself
132 is metabolite/nutrient regulated, and controlled by the amount of available glucose. The
133 distinct phases of the YMC correspondingly show a separation of metabolic processes
134 (Tu *et al.*, 2005, 2007; Murray *et al.*, 2007; Machné and Murray, 2012), and several
135 lines of evidence suggest that key metabolite amounts are critical for entering or exiting
136 a proliferative or a non-proliferative state (Murray *et al.*, 2003, 2007; Tu *et al.*, 2007; Shi
137 *et al.*, 2010; Cai *et al.*, 2011; Machné and Murray, 2012; Mellor, 2016). These studies
138 collectively indicate the following: (i) a separation of two states (proliferative, and
139 effectively G0) in cell populations, dependent on metabolic states, and (ii) a loose
140 metabolic framework within which it may be possible to study transitions between
141 quiescence and growth transitions. Thus, these studies provide extensive experimental
142 data using which a theoretical, mathematical model can be built to sufficiently explain
143 oscillations between a “quiescent” state and a “growth” state.
144
145 Here, we use existing data from these YMCs to build a robust, general model for
146 oscillations between a quiescent and a growth state. Importantly, the model
147 necessitates the requirement of a tripartite communication - between the metabolic
148 resource, the quiescent cells, and the cells exiting quiescence and entering growth - in
149 order for the cells to sustain oscillation between these two states. The model oscillations
150 depend on an underlying bistability, suggesting that cells in either state exhibit
151 hysteresis, or memory, of their states. Finally, using this model, we show how two
152 central metabolites, thought to be critical for entry into a growth state, satisfy the
153 required criteria for the currency that controls oscillations between these two cell

154 states. Collectively, we provide a coarse-grained, sufficiency model to explain general
155 principles of how cells can oscillate between a quiescent and growth state, depending
156 upon amounts and utilization of an internal metabolic currency.
157
158 **Results**
159
160 *Apparent bistable states during yeast metabolic cycles*
161
162 Yeast cells grown to a high cell density (in batch culture mode) in a chemostat, and
163 when subsequently fed limited amounts of glucose medium, spontaneously undergo
164 robust oscillations in oxygen consumption (YMCs) (Figure 1A) and (Klevecz *et al.*, 2004;
165 Tu *et al.*, 2005; Murray *et al.*, 2007; Silverman *et al.*, 2010; Burnetti *et al.*, 2015), with
166 the period of each oscillation ranging from ~2.5-5 hours (Figure 1A). For these
167 oscillations to occur, the batch culture typically needs to first be starved for a few hours
168 (Figure 1A), during which time all glucose is depleted, and all cells enter a non-dividing
169 state (although the extended starvation is not an absolute requirement, as observed
170 historically in breweries). After starvation, when cells are continuously provided limited
171 glucose in the medium, the oscillations in oxygen consumption spontaneously start and
172 continue indefinitely (Figure 1A). Comprehensive gene expression analysis across
173 these longer-period oscillations (1.5-4.5 hr cycles) has revealed highly periodic
174 transcript expression (Tu *et al.*, 2005; Rowicka *et al.*, 2007), and proteins encoded by
175 these transcripts can be binned into three general classes (Figure 1B, 1C). These
176 represent “growth genes” during the high oxygen consumption phase, followed by the
177 rapid decrease in oxygen consumption coupled with “cell division” (Figure 1B, 1C)
178 (Kudlicki *et al.*, 2007; Rowicka *et al.*, 2007). The cells exhibiting the “growth” signature
179 during the high oxygen consumption phase all go on to enter and complete the CDC
180 (42). Finally, the YMC enters a state of ~stable oxygen consumption, where the gene
181 expression profile revealed a “quiescent”-like state (Figure 1B, 1C). Mitotic cell division
182 is tightly gated only to a narrow window (Figure 1B, 1C). Interestingly, in this phase,
183 only a fixed fraction of the cells (~35%) (and not all cells) divide during each cycle
184 (Figure 1D). During the stable oxygen consumption phase, there are almost no budding

185 cells observed (Figure 1D). Note: given that this is a controlled chemostat system, the
186 overall cell number/density is constant throughout these oscillations (Klevecz *et al.*,
187 2004; Tu *et al.*, 2005), which becomes important for our mathematical model.
188
189 *Defining the two states and apparent bistability*
190
191 If these data are more grossly binned into groups, there appears to be ~2 effective
192 equilibrium states in this system. If binned based on the gene/metabolic patterns, there
193 is the oxidative phase (high oxygen consumption) closely coupled to growth,
194 immediately followed by the reductive mitotic phase, which depends upon (and follows
195 directly from), the oxidative phase. Indeed, experimental data suggest that these two
196 steps, the growth and proliferation steps, are irreversibly coupled (Laxman *et al.*, 2010).
197 This can therefore be conceived as one bin, representing a “growth” state. The
198 extended, low oxygen consumption phase where there is a long, steady build-up of
199 resources, can be viewed as a second bin. Both these states or bins appear to be
200 somewhat stable, contained systems, with what appears to be a transition or inflection
201 point leading to a committed switch to the other state. Thus, there appears to be an
202 *apparent* cellular state bistability occurring during these oscillations in oxygen
203 consumption. The stable, low oxygen consumption phase can therefore be practically
204 envisioned as representing the non-dividing, “quiescent” state (Q), while the rapid
205 increase in oxygen consumption followed by the reduction in oxygen consumption
206 phase represents the “growth” state (G) (Figure 1E). Considering this, our objective was
207 to build a mathematical model that conceptualized the oscillations in oxygen
208 consumption as oscillations between these two (Q and G) states.
209
210 For this, we first needed to define what plausible, broad scenarios this YMC system
211 might fit into. We therefore considered the currently accepted explanations for
212 commonly observed cellular heterogeneity within clonal populations. Many microbial
213 cells at high cell densities put out “quorum/alarmone” molecules that affect the entire
214 population, and lead to collective behavior along with heterogeneity (Miller and Bassler,
215 2001; Schauder *et al.*, 2001; Whitehead *et al.*, 2001; Zhu *et al.*, 2003; Chen *et al.*, 2004;

216 Farewell *et al.*, 2005; Srivatsan and Wang, 2008). Other possibilities emerge from
217 metabolic resource sharing, seen widely in systems ranging from microbial populations
218 to cancer cells (Veening *et al.*, 2008; Cairns *et al.*, 2011; Campbell *et al.*, 2015, 2016).
219 This extends to regulation at the levels of metabolic specialization and stochastic gene
220 expression resulting in phenotypic heterogeneity (Avery, 2006; Ibanez *et al.*, 2013;
221 Holland *et al.*, 2014; Ackermann, 2015; Sumner and Avery, 2017). From within this
222 range of possibilities, we envisaged three general scenarios that could result in the type
223 of oscillations (Q <-> G) seen in the YMC, and could make biological sense (Figure 1F):
224 (i) there could be the production and secretion of a resource by a sub-population of cells
225 ("feeders"), which is taken up by other cells that will go on to divide; (ii) there could be
226 the secretion and accumulation of a metabolite that is sensed and taken up by only
227 some cells (but is not consumed); (iii) there is a build up of a metabolite, which is
228 consumed by the cells at some threshold concentration (Figure 1F). Starting from these
229 scenarios, we built simple models to test which one could create an oscillatory system
230 between the two states, which can come from an apparent bistability in the system.
231

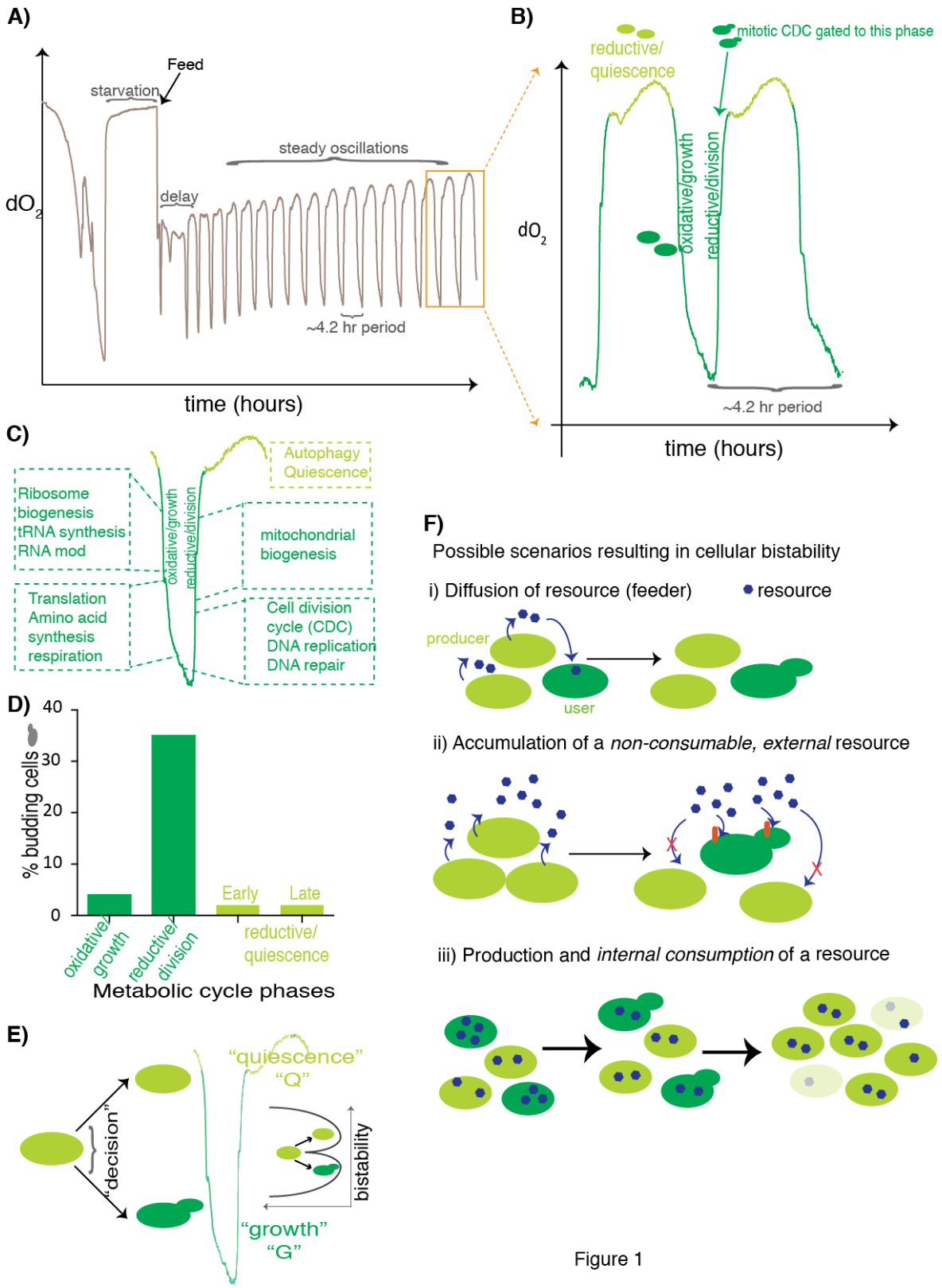

Figure 1: Apparent two-state bistability during Yeast Metabolic Cycles.

A) A representative YMC, indicating stable oscillations in oxygen consumption (based on dissolved oxygen dO2) in yeast cultures, reflecting the yeast metabolic cycle. Note that the stable oscillations are driven by restricted feeding.

B) A more detailed illustration of each oscillation cycle, also indicating the phases of the YMC.

C) Functional outputs based on gene expression studies (from (33)), which clearly define the oxygen consumption phases of the YMC into a general "growth/proliferation" phase, and a "quiescence" phase.

D) Observed cell division during the YMC. Cell division is tightly gated to a narrow window of the YMC. Note that only a fraction of cells, and not all cells, divide during this window of each cycle.

E) Reducing the oxygen consumption (dO2) oscillation into a two-state (Q state and G state) system. The apparent bistability is also illustrated.

F) Plausible biological scenarios that could result in an oscillation between Q and G states, based on observed phenomena. These scenarios are considered for building the model.

A "push-pull" model, requiring communication between the Q state, G state and the resource, produces oscillatory behavior

Model framework for a two-state yeast population

In order to model such a two-state population of cells, the variables to consider would be the following: (a) The number of cells in the quiescent state and in the growth state, (b) some indicator of resource availability (dependent on the accumulation and consumption of the resource) which could modulate the switching rate between Q and G states, and the growth rate.

Thus, using this framework, we build the following equations that can describe the dynamics of a two-state population of yeast cells in a well-mixed system:

"Change in Q population over time":

$dQ/dt = \nu_{GQ}G - \nu_{QG}Q - \phi Q$, (1)

265 “Change in G population over time”:

266 $dG/dt = \gamma G - \nu_{GQ}G + \nu_{QG}Q - \phi G$, (2)

267

268 where $Q(t)$ is the number of cells in the quiescent state at time t, $G(t)$ the number of
269 cells in the growing/dividing state, each ν represents a switching rate, $\phi(t)$ is the
270 chemostat outflux rate (which could vary with time), and γ is the growth rate of cells in
271 the growing/dividing state. If we further assume that the chemostat is working in a mode
272 that maintains the total population (or density) of cells at some constant level, i.e., the
273 outflux from the chemostat balances the growth of cells at all times, this means $\phi(t) =$
274 $\gamma G/(G + Q)$. In this case, the population dynamics can be described by a single
275 equation:

276

277 $dq/dt = \nu_{GQ}(1 - q) - \nu_{QG}q - \gamma (1 - q)q$, (3)

278

279 where $q \equiv Q/(G + Q)$ is the fraction of cells in the quiescent state.

280

281 Next, we assume that the cells contain some ‘resource’ that they require for growth,
282 without making any further assumptions about the resource. Let $a(t)$ denote the
283 concentration per cell of this resource at time t, and let σ denote the rate at which
284 additional amounts of this resource enter each cell from the surroundings (where the
285 resource is replenished due to the influx of fresh medium into the chemostat). a is
286 depleted both by dilution due to the outflux (at a rate $\gamma(1-q)$ as explained above), as well
287 as by consumption by growing cells (this rate is also proportional to $\gamma(1-q)$, which is the
288 net rate of production of new cells). The dynamics of this resource can thus be
289 described by the equation:

290

291 “Change in resource over time”:

292 $da/dt = \sigma - \mu\gamma(1 - q)a - \gamma (1 - q)a$, (4)

293

where μ is a proportionality constant that sets just how much resource is consumed by a growing cell, compared to the amount that is depleted by dilution.

In writing equations 3 and 4, we have assumed that all cells have the same amount of this internal resource *a*. A less restrictive assumption that still gives the same equation is to assume that *a* represents the average concentration of the resource across the population of cells, but that the distribution of resource levels is similar for Q and G cells. Further, the same equations also model the case where the resource is not an intracellular one, but an extracellular one - σ then is just reinterpreted as the rate at which the resource is added to the extracellular medium either by an external feed or by secretion of the resource by the cells themselves (e.g., by making σ dependent on *q*).

By choosing which of the parameters in the above equations are zero or non-zero, and how they depend on *q* and/or *a*, this framework can be used to model a variety of scenarios, which subsume the broad, biological scenarios illustrated in Figure 1E. These mathematically distinct scenarios are described below (and illustrated in Figures 2A and 2B):

1. A sub-population of feeder cells (in the Q state) secrete a resource that is sensed by other cells that can grow and divide (G state); resource accumulation σ increases with *q*.

Such a scenario can be modelled with the G cells either consuming the resource ($\mu \neq 0$), or only sensing but not consuming the resource ($\mu = 0$) in the processes of growing/dividing. The growth rate in the G state may be a constant, or may depend on the level of the resource (e.g., γ proportional to *a*). There are three sub-scenarios for how cells may switch between the two states:

a. There is no switching between Q and G states (ν_{QG} and ν_{GQ} both zero).

b. There is random switching between Q and G states (ν_{QG} and/or ν_{GQ} are non-zero constants).

c. Switching between Q and G states is dependent on cell density and/or the resource level (ν_{QG} and ν_{GQ} both functions of *q* and/or *a*).

2. All cells produce and secrete a resource that is sensed only by a sub-population of (G) cells that can grow and divide, i.e., σ is a constant. As in scenario 1, the G cells may or may not consume the resource, the growth rate in the G state may or may not depend on the level of the resource, and there are three sub-scenarios for how cells may switch between the two states: no switching, random switching or density/resource dependent switching.

3. There is a build up of a resource, which is directly supplied from outside into the chemostat medium (σ is a constant). This metabolite is sensed or consumed by the G cells when they grow/divide. Again, the growth rate in the G state may or may not depend on the level of the resource and switching may work in one of three ways: none, random or density/resource dependent switching.

While scenarios (2) and (3) may appear mechanistically very different, they are in fact mathematically no different from each other; both result in a constant production of the resource (Figure 2B). Hence, we need not distinguish between these two. Testing all the scenarios above, using equations 3 and 4, we show in the next section that oscillations are not possible in the absence of switching, or even with random switching, when there is no substantial time delay between resource utilization and division events (as assumed in writing equations 3 and 4). Thus, scenarios 1c, 2c and 3c are the only possibilities left that give oscillations (Figure 2C). This means that the switching between Q and G states is a stochastic event, but with a probability that depends on the resource level, and/or the density of cells in the Q or G state, implying some form of communication between the resource, the cells in the Q state and the cells in the G state.

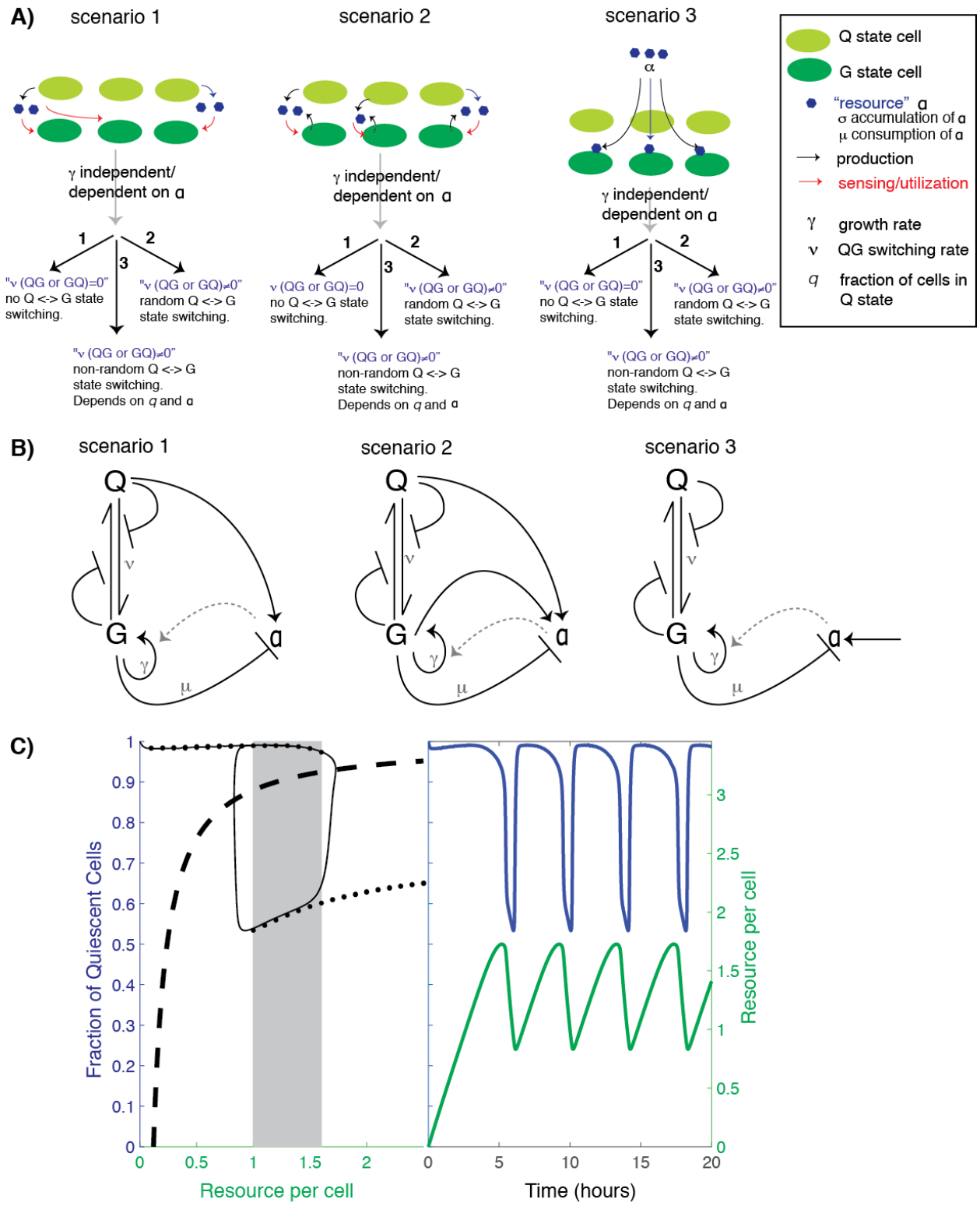

Figure 2

Figure 2: A "push-pull" model for oscillations arising from an underlying bistability between Q and G states.

A) A range of biologically plausible scenarios from Figure 1F, now broken down into precise categories, where parameters affecting the rates of proliferation (g), switching between Q and G states (n), as well as consumption (m) and supply (s) of the resource are included. The variations in these parameters are used to build and test our model.
B) Schematic illustration of Figure 1A, indicating feedback loops and parameters considered, to test for possible oscillations between Q and G states. For clarity, potential feedback loops caused by the parameters being dependent on the resource a are not shown, but are included in our models.
C) A hysteretic oscillator, based on switching between Q and G states, a required communication between Q, G and the resource, and the oscillation of the amounts of resource itself that controls the Q<->G transitions (see the Methods for the parameter values that that produce this dynamics). In the left panel: The thin black curve shows the path traced by the oscillation in the q-a plane, the thick dashed line is the curve along which production of resource exactly balances consumption/dilution, and the solid black dots trace the high and low branches of the steady state q levels when the resource level is held constant (the grey rectangle indicates the region of bistability). In the right panel: blue and green curves show, respectively, the fraction of quiescent cells and the resource level as a function of time.

Some necessary conditions for oscillations

Within the framework of our model we can show that a density-dependent switching rate is necessary to get oscillations.

(i) *No oscillations in the absence of switching:*
When both ν_{QG} and ν_{GQ} are zero, then equation 3 above becomes:
$dq/dt = -\gamma(1 - q)$. (5)
As long as γ is always positive, irrespective of its dependence on a, this has only one stable steady-state solution, $q = 0$, because the rate of change of q is always negative. And this is globally stable, i.e., every initial value of q (except $q = 1$) will flow to $q = 0$. The $q = 1$ state is an unstable steady state, i.e., any fluctuations away from it, however small, will result in the system moving to $q = 0$. Thus, there can be no oscillations in the absence of switching.

(ii) *No oscillations with constant parameters:*

When all the parameters in equations 3 and 4 are constants, independent of *q* and *a*, then no oscillations are possible because eq. 3 becomes independent of eq. 4, and therefore, being a one dimensional ordinary differential equation without explicit time-dependence, cannot show oscillations (an oscillation in *q* requires that *dq/dt* take both positive and negative values for the same value of *q*, for at least within some range of *q*, and this is not possible for a 1D ordinary differential equation).

(iii) *No oscillations for random (density-independent) switching:*

A less restrictive assumption is that ν_{GQ} and ν_{QG} are constants (which includes zero - we've already examined the case where both are zero above), but γ and σ may be functions of *q* and/or *a*. In the scenarios we examine, γ may be an increasing function of *a* (all scenarios), while σ may be an increasing function of *q* (scenario 1). In this situation, the dependence of each variable on the other is `monotonic' (*dq/dt* is a decreasing function of *a*, while *da/dt* is an increasing function of *q*). Equations with such monotonic dependencies have been studied mathematically in detail (Pigolotti *et al.*, 2007; Tiana *et al.*, 2007), which show explicitly that when such a coupled set of equations has only two variables (here, *q* and *a*), then sustained oscillations are not possible. Intuitively, there is not enough time delay in such a small two-leg feedback loop to destabilise the overall negative feedback that pulls the variables into a single stable steady-state value.

Hysteretic oscillator based on the two-state model

Apart from there being broadly two states, a second crucial observation from the experiments is that there is a distinct separation of timescales. The transitions from a situation where almost 100% of cells are in the Q state to one where 30-40% are in the G state, and vice versa, are very rapid. Whereas, between these two transitions the dynamics proceeds on much slower timescales. A simple way to obtain such a two-timescale oscillator from this two-state model uses the strategy of `frustrated bistability' previously suggested by (Krishna *et al.*, 2009). It requires three ingredients: (1) a

negative feedback loop between *q* and *a*, (2) bistability in *q* in the absence of the feedback, and (3) the assumption that changes in *q* happen on a relatively fast timescale compared to changes in *a*. While the first can be achieved in several ways, the two simplest, biologically plausible, scenarios are where growing cells consume a resource *a* and: (i) the growth rate γ is proportional to the resource *a*; or, (ii) one or both switching rates depend on *a* such that the net switching rate from G to Q decreases with *a*. However, the third requirement of separation of timescales means that the switching rates must be at least several-fold higher than γ and σ. This means that the term $\gamma q(1-q)$ in equation 3 is practically negligible and hence the dependence of γ on *a*, or lack of it, would have little effect. We therefore concentrate on the case (ii) where the switching rates depend on *a* to implement the negative feedback, and for simplicity keep γ independent of *a*.

Bistability in *q* in the absence of the feedback implies that when *a* is kept fixed, for some range of *a* values, equation 3 should allow two stable steady state levels of *q*, one lower and one higher. This is shown in Figure 2C left panel, where one can see the high and low 'branches' traced by the solid black circles - every point on these branches is a stable steady state *q* can attain for the corresponding *a* value, using a version of equation 3 derived from scenario 3 in Figure 2B (see Methods for the full equation). When the resource *a* is sufficiently small, then there is only one high steady-state level possible for *q*. Similarly, when *a* is sufficiently large, there is only one low steady-state possible. However, for intermediate values of *a*, the system exhibits bistability and both low and high steady-state levels co-exist. In this bistable region, which steady-state level *q* attains depends on where it started (i.e., its 'initial condition'). Importantly, in these oscillations, the system exhibits a 'memory' (or a 'hysteresis') - the steady-state level that *q* eventually settles into depends on the history of the system.

When there exists such bistability, then one can get oscillations from the system described by equations 3 and 4, provided the switching rates are a few-fold faster than the rates of consumption and accumulation of the resource (Krishna *et al.*, 2009), as follows: when *q* is high, *a* increases due to lack of consumption, so the system creeps

447 along the high branch in Figure 2C left panel (see the trajectory traced by the thin black
448 line) until it hits the edge of the bistable region. At that point, cells start switching to the
449 G state, which happens relatively rapidly due to the separation of timescales. Thus, the
450 trajectory "falls off" the edge down to the low branch. On the low branch, with more G
451 cells, the now increased consumption of the resource causes *a* to start decreasing,
452 leading to the system creeping down along the low branch. When the system reaches
453 the left edge of the bistability, the trajectory jumps up to the high branch as cells rapidly
454 switch to the Q state. For a range of parameter values, this settles into a stable
455 oscillation, as shown in Figure 2C right panel, which shows how *q* and *a* vary with time
456 as one follows the black trajectory in Figure 2C left panel.
457
458 For this kind of oscillation, as we have demonstrated in the previous section, ν_{QG} and/or
459 ν_{GQ} must necessarily be functions of *q*, not constants independent of *q*. This can be
460 interpreted as a form of '*quorum/cell number sensing*' - implying some form of cell-cell
461 communication (or a cell density dependent phenomenon). More specifically, we find
462 that choosing either ν_{QG} to be a decreasing step-function of *q* (as in Figure 2C), or ν_{GQ}
463 to be an increasing step-function of *q* (see Supplemental Figure S1) is sufficient to
464 produce frustrated bistability. Other shapes that we have not explored may also produce
465 bistability, and hence oscillations. However, our purpose here is not to find the 'best-fit'
466 model, but rather to demonstrate the basic ingredients which are sufficient to produce
467 hysteretic oscillations that are similar to the experimental observations. The requirement
468 for ν_{QG} to be a decreasing step-function of *q*, or ν_{GQ} to be an increasing step-function of
469 *q*, is basically a requirement for a "push-pull" mechanism - the more the Q cells, the
470 more other Q cells get pulled to remain in that state, and the more G cells get pushed to
471 switch away from their state, and vice versa. Irrespective of the precise molecular
472 means by which this is achieved, cell-cell communication is a necessary ingredient for
473 implementing such a push-pull mechanism.
474 *Possible variations in the shape of the oscillations*
475
476 From our gross model explained in Figure 2, we obtain predictable oscillations with a
477 specific pattern. The model oscillations exhibit a fast drop in *q* when exiting the

478 predominantly quiescent phase, followed by a slow(er) drop, and then a rapid rise back
479 to a high *q* level. Experimentally however, a few variations within the general oscillation
480 patterns are known to occur, depending upon the strain background (Burnetti *et al.*,
481 2015). In the CEN.PK strain (our major reference system, from where the gene and
482 metabolite oscillation datasets were obtained (Tu *et al.*, 2005, 2007; Mohler *et al.*,
483 2008)) dO2 levels (which we equate with *q*) show a fast drop, a slow further drop, and
484 then a rapid rise (Figure 3A scenario (i)). However, as comprehensively described in
485 (Burnetti *et al.*, 2015), three other variations have been extensively documented.
486 Following a fast drop in dO2 levels, some strains then show a slower drop followed by a
487 more extended low dO2 phase (bump), and a fast rise in dO2 (Figure 3A, scenario (ii)).
488 Other strains show an overall fast drop in dO2, an extended low dO2 phase and bump,
489 and a fast rise (Figure 3A, scenario (iii)), or a fast drop in dO2 (increased oxygen
490 consumption), followed by a slower, extended rise in dO2 (Figure 3A, scenario (iv)).
491
492 *Can our model explain this small diversity of shapes seen during the overall drop and*
493 *rise in oxygen concentrations?*
494
495 In the model, the shape observed depends on the shapes of the two branches of *q*
496 steady-states (solid black circles in Figure 2C, left panel). Because the lower branch
497 starts at a *q* value of around 0.5 and then increases as *a* increases, therefore there is a
498 slow drop in *q* after the fast drop. To produce the experimental dO2 oscillations in other
499 yeast strains (as shown in Figure 3A), the lower branch must have a different shape.
500 For example, for strains which show a slow increase after the first rapid decrease of *q*,
501 the low *q* branch must *decrease* as *a* increases. Similarly, the other waveforms would
502 involve other shapes of the lower or higher branches. In Figure 3C we show that simple
503 changes in the dependence of the switching rate ν_{QG} on *a* produce different waveforms
504 for the oscillations. Here we've shown how to get different shapes of the low-*q* phase of
505 the oscillation by manipulating the lower branch of the bistability - changes to the high-*q*
506 phase could similarly be easily made by manipulating the upper branch. The main point
507 is that the shape of the waveform is primarily determined by the shape of the bistability
508 branches, which in turn are determined by how ν_{QG} and ν_{GQ} depend on *q* and *a*. Thus,

our model predicts that these switching rates are what must vary between strains that show different oscillation waveforms.

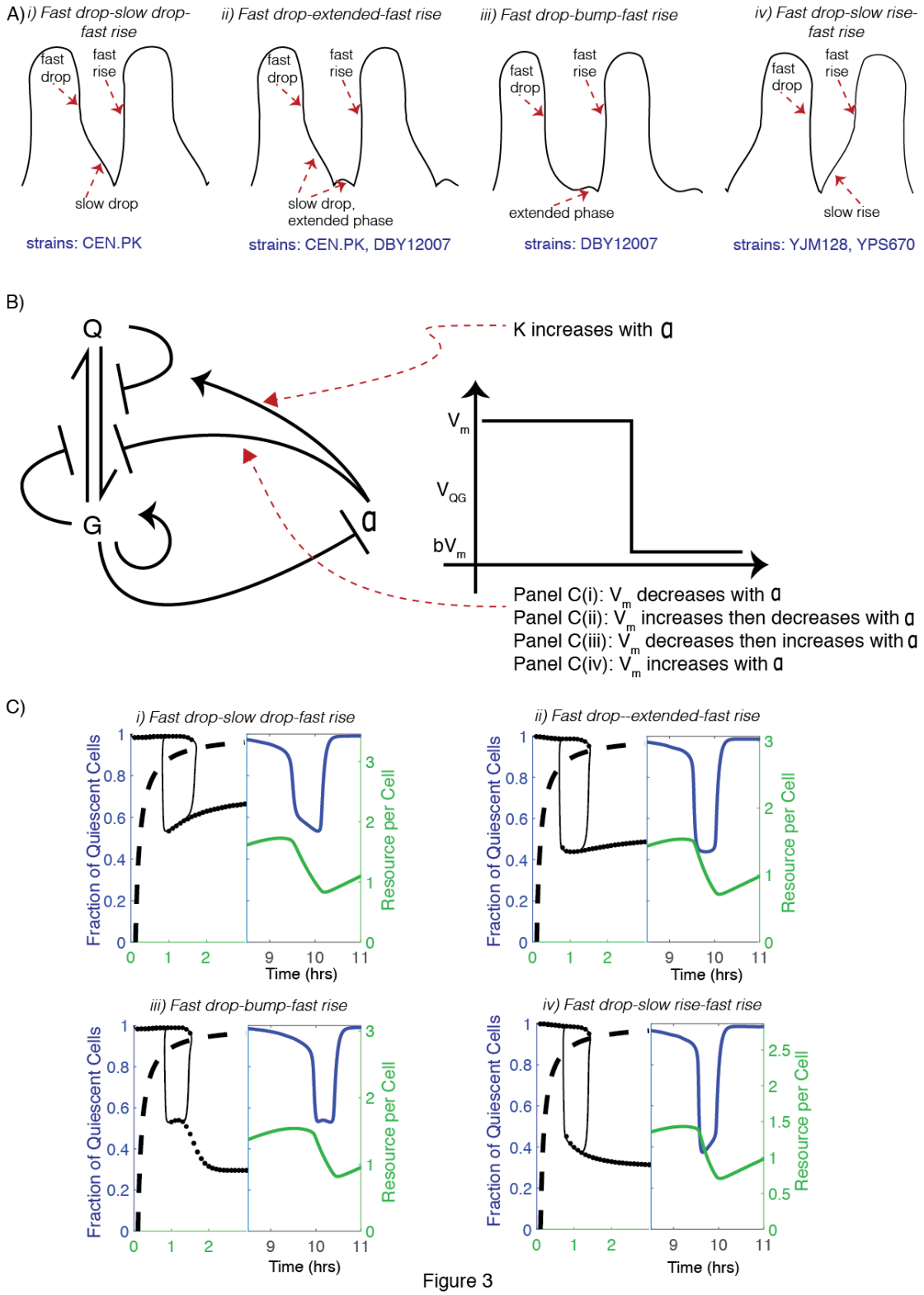

Figure 3

512 *Figure 3: Diverse waveforms in the oscillations: experimentally observed and model predictions.*
513 *A) Experimentally observed patterns of oscillations in dissolved oxygen/ oxygen consumption, which is*
514 *dependent on yeast strain backgrounds and chemostat growth conditions.*
515 *B) Altering the communication loops between Q, G and a, to change the overall oscillation waveform.*
516 *Here g (growth rate) is constant and n_{QG} is a decreasing step-function of q. To obtain different*
517 *waveforms, we vary the way the step function parameters n_m depends on a.*
518 *C) Predicted oscillation patterns from the model (as altered described in panel B). The illustrated panels*
519 *cover the range of waveforms observed experimentally in panel A. (i) same as Fig 2C; n_m decreases with*
520 *a. (ii) n_m first increases then decreases with a. (iii) n_m first decreases and then increases with a. (iv) n_m*
521 *increases with a. Additionally, in all four cases, K increases with a and other parameters have been*
522 *chosen so that the time period of oscillations is close to 4 hours (see Methods for the full equations, with*
523 *parameter values, for each case).*
524
525 *Predicting oscillatory outcomes based on resource availability*
526
527 We have used scenario 3c (from Figure 2) to produce oscillations in Figures 2 and 3
528 above. We reiterate that mathematically scenarios 2 and 3 are the same, so scenario 2c
529 can produce exactly the same oscillations. Further, we also find that scenario 1c (where
530 the resource is not supplied externally, but produced/secreted by only the Q cells) is
531 also capable of producing similar oscillations, based on highly constrained choices for
532 how the production rate of the resource (σ) depends on *q* and *a* (see Supplemental
533 Figure S2). Thus, while scenarios 3c and 2c are identical, all three scenarios, 1c, 2c, 3c,
534 with appropriate choices for how the switching rates, and production and consumption
535 depend on the resource and fraction of quiescent cells, are sufficient to explain the YMC
536 oscillations. Scenario 2c and 3c are largely indistinguishable, and both appear
537 biologically most plausible. Given our experimental understanding of the YMC (and the
538 need for a consumable resource, glucose, to control the oscillations), we think scenario
539 3c is most likely (and we will explore this further in a subsequent section).
540
541 **Breakdown of the oscillations.**
542

543 In Figures 2 and 3 above, we have chosen the particular “default” values of each of the
544 model parameters such that the oscillation period became approximately 4 hours, to
545 match the experimental observations in Figure 1. Of course, varying these parameter
546 values changes the time period, and for large enough variation the oscillation may also
547 disappear. Our model predicts how the oscillation shape and period will vary, and when
548 oscillations will break down, in response to experimentally tunable parameters. For
549 instance, Figure 4A shows how the oscillations change as the resource production rate,
550 σ, is varied around its default value, for the same equations that produced the
551 oscillations in Figures 2 and 3. When σ is decreased below the default value, the
552 oscillation period initially increases, with more time being spent in the high-*q* phase. For
553 low enough σ, the model exhibits damped oscillations, and then as σ is lowered further,
554 the model exhibits the absence of oscillations, with *q* settling into a high steady-state
555 value (see Figure 4A, and also Supplemental Figure S3 for more such plots). When σ is
556 increased from its default value, we again find that the period initially decreases, with
557 less time being spent in the high-*q* phase. We are able to produce oscillations having a
558 time period as low as ~2.5 hours (see Figure 4A(iii)). When σ is increased beyond this,
559 the oscillation period starts increasing again, and the low-*q* phase of the oscillation
560 starts becoming pronounced (see Supplemental Figure S3). Eventually, the oscillations
561 disappear, with *q* settling into a (relatively) low steady-state value. These predictions
562 largely mirror known experimental observations, where decreasing or increasing feed
563 rate (at these scales) control oscillations similarly.
564
565 The resource production rate σ is a parameter that can be tuned relatively easily in a
566 chemostat by controlling the amount of fresh glucose or ethanol being supplied per unit
567 time. However, another parameter that may be tunable by genetic modifications is γ, the
568 growth rate of cells when they are in the G state. Figure 4B shows how the oscillations
569 vary as γ is varied. The results are qualitatively similar but inverse to what was observed
570 with σ variation - an increase in γ from the default value results in an increasing period,
571 damped oscillations and eventually no oscillations, while a decrease first results in a
572 decrease of period, then a distorted shape and increasing period (see Supplemental
573 Figure S4 for more such plots).

The location of the dashed black lines in Figure 4 (left panels) help to understand this behaviour. Each dashed line traces the *q* and *a* values where resource production exactly balances resource consumption/dilution. To the right of the line the production is less than the consumption so the resource must decrease, and vice versa to the left of the line. The closer one is to the dashed line, the slower the rate of change of *a*. As explained in (Krishna *et al.*, 2009), oscillations occur only when this dashed black line passes between the upper and lower bistable branches (solid black circles) - because then the resource keeps increasing (decreasing) when it reaches the end of the high (low) branch making the trajectory “fall off the edge” and continue the oscillation. When σ is decreased the dashed black line shifts leftward in the plot, coming closer to the high *q* branch which causes the oscillating trajectory to spend more and more time on the high *q* branch (because it is closer to the dashed line and so the resource accumulates slower). Eventually, as the dashed line just touches the high *q* branch, the time period of oscillations increases to infinity (logarithmically – see Supplemental Figure S5). For σ values lower than this critical value there is no sustained oscillation and the system settles into a steady-state on the high branch at the point where it crosses the dashed line. A similar behaviour happens as σ is increased and the dashed line comes closer to the lower branch, with the only difference being that the oscillating trajectory spends more time at lower *q* values.

A universal feature of the YMC oscillations seen in diverse yeast strains is that the time period of the oscillations decreases with an increase in the dilution/supply rate in the chemostat. The time period appears to be dominated by the time spent in the high-*q* phase, which also increases with dilution/supply rate, whereas the time spent in the low-*q* phase is less and *decreases* slightly with increase in the dilution/supply rate (described in (Burnetti *et al.*, 2015)). As described above, in our model, we find that as we vary σ or γ, there are two regimes. In one the time period is dominated by the high-*q* phase, and the behaviour matches the above experimental observations (see Supplemental Figure S5). However, there is also another regime, where the time period is dominated by the low-*q* phase. Our model therefore predicts that: (i) the observed

YMC oscillations are closer to the lower end of the σ range that produces oscillations, so one should be able to increase σ more than decrease it before breaking the oscillations, and (ii) if one increased σ enough while remaining in the oscillatory regime one should observe low-*q* dominated oscillations such as those shown in Supplemental Figure S3. These are both testable predictions of our model.

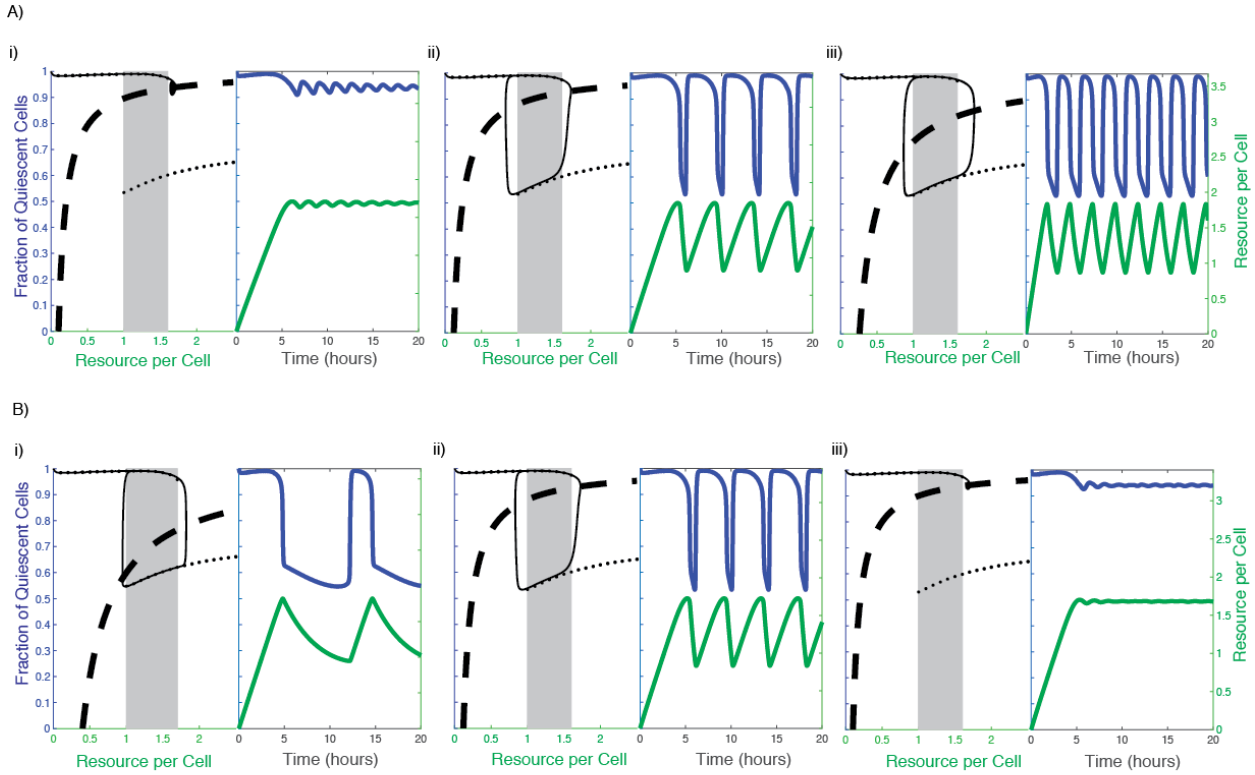

Figure 4

Figure 4: Breakdown of oscillations.

A) Varying the rate of production of resource σ. (i) σ = 0.346 hr, (ii) σ = 0.400 hr (default parameters, same as Figure 3), (iii) σ = 0.866 hr.

B) Varying the growth rate of cells γ. (i) γ = 0.500 hr, (ii) γ = 1.665 hr (default parameters, same as Figure 3), (iii) γ = 2.000 hr. Equations used, and other parameter values, are the same as those that produced Figs 2C and 3C(i).

Acetyl-CoA and NADPH satisfy the requirements of the consumable resource that controls oscillations between Q and G states

Based on our model, the metabolic resource oscillates with a unique pattern, and this

drives the oscillation between the Q and G states. From the model, some resource builds up within the cell, and is highest at the point of commitment to the switch to the G state (Figure 5A). It is then rapidly consumed/eliminated to fall below a certain threshold, resetting the oscillation, after which the cycle of building up for consumption resumes. When superimposed to the actual YMC phases (and the Q to G switch), this build-up of the resource would necessitate its highest amounts at the beginning of the phase where cells commit to entering high oxygen consumption (Figure 5A). We note that these features of the resource oscillation are a very robust prediction of our model. Across all the oscillations in Figs 2-5 we see the same behaviour, and we would see this for any parameter choice that gives oscillations because this behaviour depends only on our assumption that the resource is consumed by growing/dividing cells and not by quiescent cells. Therefore, according to our model, in order for any metabolite to be the resource that controls the oscillation between the two states, this molecule must fully satisfy the above criteria. Furthermore, for completing this switch to the G state, the metabolite must be able to drive all the downstream biological events for growth. So do any central metabolites satisfy these requirements, and could therefore be the internal resource that controls these Q-G oscillations?

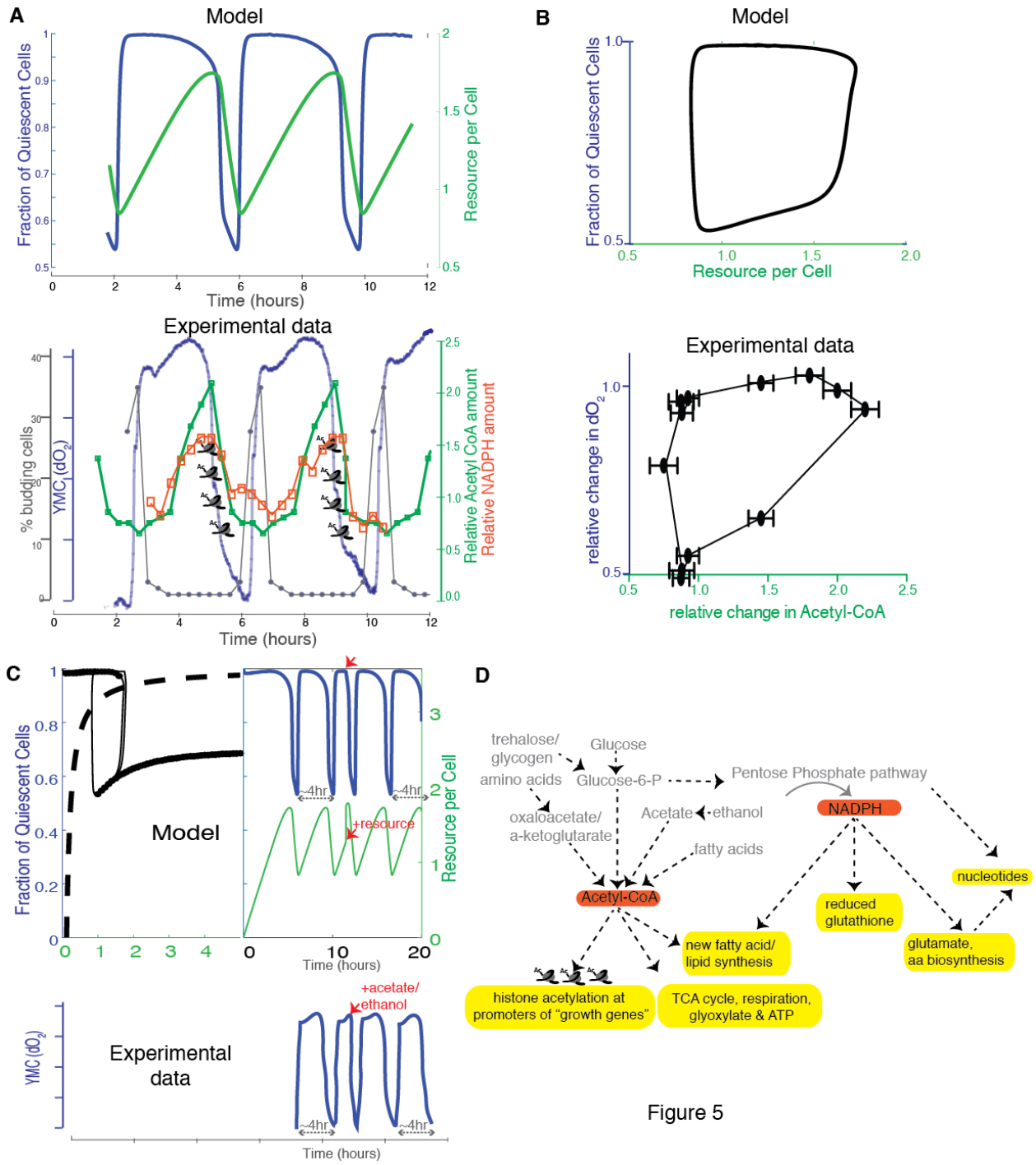

Figure 5

Figure 5: Acetyl-CoA satisfies the requirements for the metabolic resource controlling the Q and G oscillations.

A) Predicted pattern of oscillation of the resource, during the Q and G oscillations, based on the model (top panel, same oscillations as Figure 2C), and experimentally

645 *observed oscillations of acetyl-CoA and NADPH during the dO2 oscillations (bottom*
646 *panel).*
647 *B) Predicted phase portrait of the the fraction of quiescent cells vs the resource per cell*
648 *based on the model (top panel), and experimentally observed oscillations in dO2 and*
649 *acetyl-CoA.*
650 *C) Predicted effect on the oscillation waveforms and the Q and G states, when a bolus*
651 *of the resource is added to cells in the Q state (see Methods for details), vs*
652 *experimentally observed data on oxygen consumption when a resource, acetate (the*
653 *trace is similar with for resources like ethanol, acetate, acetaldehyde, glucose) is added*
654 *to cells in the low oxygen consumption phase. Supplemental Fig S6 shows how the*
655 *response varies as the time of adding the bolus is varied.*
656 *D) Acetyl-CoA as a central regulator of a switch to the growth (G) state. The schematic*
657 *illustrates a cascade of biological processes leading to growth that acetyl-CoA amounts*
658 *regulate (coupled with coincident, required NADPH utilization). Note that all resources*
659 *that reset the oscillations, as indicated in (C) are utilized after they are converted to*
660 *acetyl-CoA.*
661
662 Comprehensive datasets of 50-100 oscillating metabolites in the YMC exist (Murray *et*
663 *al.*, 2007; Tu *et al.*, 2007; Mohler *et al.*, 2008). From these studies, the oscillations of
664 only two metabolites, acetyl-CoA and NADPH, fully fit the criteria demanded by our
665 model. The acetyl-CoA and NADPH oscillations as a function of the metabolic cycle,
666 and transitions between the Q and G state are shown in Figure 5A and 5B. The
667 oscillations of acetyl-CoA during the YMC almost perfectly superimposes with the
668 oscillation pattern of the hypothetical metabolic resource predicted by the model (Figure
669 5A). We plotted phase diagrams of the fraction of quiescent cells vs the amount of
670 resource in the cell (from the model), and also plotted phase diagrams from
671 experimental data for the dO2 oscillations plotted against acetyl-CoA amounts (Figure
672 5B). The two phase diagrams (from the model, and from experiments) strikingly
673 resemble each other (Figure 5B). This is despite the fact that the experimental data for
674 acetyl-CoA is of low resolution, with only a few sampling/time points covered, and also
675 only reflects overall (bulk population) measurements of acetyl-CoA, suggesting that the

676 actual phase diagram might be even more similar. Thus the model appears to capture
677 key universal features of these yeast oscillations, including the point of exit from low
678 oxygen consumption (Q) to high oxygen consumption and back (G), and the parameters
679 important in the waveform (i.e. the low and high oxygen consumption phases are
680 important, while the precise form of the dip and increase in dissolved oxygen may not
681 be so). The model also supports an inference that the acetyl-CoA oscillations are
682 sufficient to explain the bistability between the Q and G states, and retains the
683 hysteresis component.
684
685 Using our model, we next simulated what would happen if the resource was increased
686 to just above the threshold level, at a different time. In our model, during normal
687 oscillations, the amount of resource steadily increases, while the cells are in the Q state.
688 In our simulation, we provided a single bolus of the resource, while cells were in the Q
689 state (Figure 5C). We observed a predictable, sharp exit from the Q state and entry into
690 the G state (Figure 5C), effectively resetting the oscillation, which then continued and
691 restored itself to the normal, ~4 hour period in the next cycle. We compared this to
692 available experimental data, where oscillations have been reset by adding a bolus of an
693 external agent, typically glucose, acetate, acetaldehyde or ethanol (Murray *et al.*, 2003;
694 Klevecz *et al.*, 2004; Tu *et al.*, 2005; Cai *et al.*, 2011). All these agents show near-
695 identical patterns of resetting of oscillations (exit from Q and entry into G), and a
696 representative figure (for acetate addition) is shown in Figure 5C. Here, cells exit the
697 low oxygen consumption phase and enter and exit the high oxygen consumption phase,
698 and subsequently quickly restore normal (in this case ~4 hr) oscillations. This simulation
699 can be done in any part of the oscillation, and whenever most cells are in Q, adding a
700 bolus of the resource similarly resets the oscillation (Supplemental Figure S6). Also
701 notably, adding this resource when cells have switched to the G state does not alter the
702 oscillations much (Supplemental Figure S6), which is also something widely established
703 in experiments. Thus, the oscillations predicted by the model very closely recapitulates
704 the patterns of oscillations observed in experiments, how the central, controlling
705 resource might oscillate, and how the oscillations are affected upon perturbing the

706 resource. This strongly suggests that the threshold amounts of the resource are
707 sufficient to set the oscillations and switching between Q and G states.
708
709 Multiple lines of experimental data suggest that these two metabolites, acetyl-CoA and
710 NADPH, are key in controlling exit from quiescence and entry into growth (Tu *et al.*,
711 2007; Cai *et al.*, 2011; Cai and Tu, 2012; Machné and Murray, 2012; Shi and Tu, 2013,
712 2014; Mellor, 2016). Based on our knowledge of the metabolic prerequisites for entering
713 growth, and known functional endpoints or outcomes of these two molecules (Figure
714 5D), we can now make a strong, parsimony based argument suggesting that oscillations
715 in these two metabolites are sufficient to control oscillations between the Q and G state.
716 Particularly, several lines of study suggest that the entry into growth (from quiescence)
717 depends on carbon source utilization (Shi *et al.*, 2010; Cai *et al.*, 2011; Daignan-Fornier
718 and Sagot, 2011; Laporte *et al.*, 2011). As pointed out earlier, studies from the yeast
719 metabolic cycle show that the oscillations depend upon carbon sources (primarily
720 glucose) (Klevecz *et al.*, 2004; Tu *et al.*, 2005), and oscillations can be reset (to enter
721 the growth program) by adding acetate, acetaldehyde, etc. (Murray *et al.*, 2003; Tu *et*
722 *al.*, 2005; Cai *et al.*, 2011). Notably, these carbon sources end up being converted
723 directly to acetyl-CoA, and can only then be utilized (Figure 5D). Additionally, a growth
724 program will require not just sufficient energy (ATP) to sustain the anabolic processes
725 within it, but also activate a program boosting anabolic processes that lead to cell
726 division, including making enough lipid moieties required for cell membranes and other
727 constituents of a new cell. Notably, acetyl-CoA satisfies all these requirements in the
728 following manner (Figure 5D): it directly enters the TCA cycle to generate ATP (Nelson,
729 DL; Cox, 2017); it can be utilized for the biosynthesis of numerous cellular metabolites,
730 including fatty acids, sterols, and amino acids (Nelson, DL; Cox, 2017); and directly
731 regulates cell growth and ribosome biogenesis by the acetylation of histones at “growth
732 promoting genes”, especially histones at ribosome subunit, tRNA and ribi genes, and
733 activates their transcription by the SAGA complex (Cai *et al.*, 2011). The genes that
734 breakdown storage carbohydrates (such as glycogen and trehalose) that produce
735 acetyl-CoA all peak before the maximal acetyl-CoA concentration (Tu *et al.*, 2005;
736 Kudlicki *et al.*, 2007). Finally, the exit from quiescence requires the liquidation of these

storage carbohydrates (Shi *et al.*, 2010; Laporte *et al.*, 2011; Shi and Tu, 2013), and conversion to acetyl-CoA (and the subsequent gene expression program) (Shi and Tu, 2013). Perturbations in the ability to sense and utilize acetyl-CoA (particularly for the gene expression program) completely abolish oscillations (Cai *et al.*, 2011). Physiologically, this anabolic commitment also absolutely requires the process of reduction for anabolic biosynthesis, and this reductive capacity is supplied by NADPH (Nelson, DL; Cox, 2017) (Figure 5D). NADPH is primarily synthesized from the pentose phosphate pathway, which branches from this same central carbon network, and this NADPH will fuel the required reductive biosynthesis to make molecules required for anabolism (Figure 5D). Finally, genes encoding proteins that increase the synthesis of NADPH are similarly coincident with those that lead to the generation of acetyl-CoA, and disrupting NADPH production slightly results in a collapse of oscillations (Tu *et al.*, 2005, 2007). Relatedly, studies from the YMC show multiple other metabolite oscillations coupled to or dependent upon NADPH, although any hierarchical organization was not immediately apparent (Murray *et al.*, 2007). Without a necessary coupling of the two molecules, the overall process of entry to growth cannot be completed. There is substantial data, particularly from the studies of various cancers, to show the close coupling of acetyl-CoA and NADPH for growth (Heiden *et al.*, 2009), as well as direct evidence of acetyl-CoA promoting NADPH synthesis (Patra and Hay, 2014; Shan *et al.*, 2014). Summarizing, based on the pattern of oscillation of the resource predicted by our model, acetyl-CoA and NADPH (based on production and utilization) satisfy sufficiency requirements to be the molecules that control the Q-G state oscillations. Our model thus strongly supports an argument for oscillations in acetyl-CoA being sufficient to control Q-G state oscillations.

Discussion

In this study, we present a simple frustrated bistability model to explain how the amounts of an internal metabolic resource can determine oscillations between a quiescent and growth state. For this, we relied on extensive data coming from the YMC, and represented the oscillations in dissolved oxygen (seen during YMCs) as a reflection

768 of growth and quiescent states (Figure 1). Our model incorporates factors dependent on
769 growth rate and amounts of the resource, as well as switching rates (between the G and
770 Q states). Importantly, the model emphasizes a necessary communication between the
771 cells in the quiescent state and the growth state, both of which interact with the
772 metabolic resource during such transitions (Figure 2). Quiescent cells “push” cells in the
773 growth state into quiescence, and “pull” other quiescent cells to remain quiescent, with
774 the feedback requirements imposed by the resource being distinct and opposite for the
775 Q and G states. Given this communication requirement between the Q and G states,
776 our model suggests that such oscillations will eventually breakdown when the cell
777 numbers are small and cells are no longer in contact with each other (something that
778 has been experimentally observed (Laxman *et al.*, 2010)). This model also provides
779 insight into understanding the “growth/division” rate of cells once committed to growth.
780 While healthy debates continue on the rate of growth in a cell and stages of the cell
781 cycle (Johnston *et al.*, 1977; Conlon and Raff, 2003; Jorgensen *et al.*, 2004; Brauer *et*
782 *al.*, 2008; Goranov *et al.*, 2013). our model shows that it is sufficient for oscillations to
783 have a fixed “growth rate” once the metabolic resource has crossed its threshold
784 concentration, and triggered a committed growth program, after which the growth and
785 division process is no longer dependent on available nutrients. This is also analogous to
786 studies of the CDC, which are built around committed, “no return” steps that proceed at
787 constant, predictable rates once committed to. In our model, because there is a
788 timescale separation between growth and switching rates, making the growth rate
789 dependent on the resource would make some quantitative difference to the rate of
790 accumulation/consumption of the resource, but would leave the Q-G oscillations largely
791 unchanged. Finally, using a parsimony based argument, we suggest that acetyl-CoA
792 (along with NADPH) satisfies all requirements for the resource that drive these
793 oscillations between the Q and G states (Figure 5). With acetyl-CoA as a resource, our
794 model, which builds oscillations on an underlying hysteresis, reproduces universal
795 features observed in these yeast metabolic oscillations, and provides a fairly simple
796 sufficiency argument for how cells transition between Q and G states. We reiterate that
797 our model only provides a paradigm to explain how the oscillations in an internal
798 metabolic resource is sufficient to control oscillations between quiescent and growth

states. This allows for (but doesn't include) other necessary elements in cells (e.g., unique gene transcription programs, or subsequent metabolic events that typically must follow), that may also be required to build a more detailed model for Q-G oscillations.

The kind of oscillator we have built falls under the class of "relaxation oscillators", which have been used to model a very wide variety of phenomena, ranging from electronic oscillations to oscillating chemical reactions (Balthasar, 1926; Strogatz, 1994). These are a subset of several possible types of oscillators that arise in biological systems, and are especially relevant for the CDC (Novák and Tyson, 2008; Tsai *et al.*, 2008; Ferrell *et al.*, 2009; Ferrell, 2011). Relaxation oscillators typically involve the cyclic slow build-up of some quantity, like charge in a capacitor, until it reaches a threshold level which then triggers a "discharge" event, resulting in a rapid drop of the quantity. Thus, relaxation oscillators are often characterised by processes happening on two very different timescales, with the time period mainly determined by the slow process (Tyson *et al.*, 2003; Novák and Tyson, 2008; Tsai *et al.*, 2008; Ferrell *et al.*, 2009; Ferrell, 2011). This is why, in contrast to linear, harmonic oscillators, they can produce non-smooth oscillations like a square or sawtooth waveform. We note that the YMC oscillations show a clear signature of multiple timescales - in Figure 1 it is evident that the exit from quiescence (fast drop in dO2), as well as the re-entry into quiescence (fast rise in dO2), happen at much faster timescales than the other phases of the oscillation. In our relaxation oscillator model of the YMC, these differing timescales arise from the fact that the switching rates are an order of magnitude larger than the rates of production and consumption of the resource, and even the growth rate of the cells. The latter processes are therefore what determine the time period of the YMC. Within the class of relaxation oscillators, our models fall into a sub-class that depends on an underlying bistability, which is 'frustrated' (Krishna *et al.*, 2009). The bistability, and the resultant hysteresis, are what determine the threshold points at which the behaviour of the system rapidly switches between accumulating or consuming the metabolic resource. Interestingly, our model necessitates this strong hysteresis element within the Q and G state cells. The phenomenon of hysteresis has been extremely well studied (and established) particularly during many phases of the classical CDC, or proliferation cycle ((Pomerantz

830 and McCloskey, 1990; Tyson and Novak, 2001; Solomon, 2003; Wei *et al.*, 2003; Angeli
831 *et al.*, 2004; Han *et al.*, 2005; Ferrell *et al.*, 2009; Ferrell, 2011; Yao *et al.*, 2011) and
832 many more). In contrast, a hysteresis phenomenon has not been extensively explored
833 when cells transition between a growth state and an effective quiescence state. Yet, in
834 such conditions where the transition between the two states is substantially determined
835 by a metabolic oscillator, as seen in the YMC and several other studies from simple
836 models like yeast, the hysteresis phenomenon is clearly revealed by our model. Given
837 this, experimental studies can be designed to dissect the nature of this hysteresis
838 phenomenon.
839
840 *General features emerging from the model to understand oscillations between*
841 *quiescence and growth:*
842
843 Although our model is relatively simple, uses data from a fairly elementary system, and
844 makes minimal assumptions, it does surprisingly well to constrain the possibilities for
845 how transitions between quiescence and growth are regulated. The model successfully
846 captures universally observed waveforms of oscillations, can reset the oscillations, can
847 predict how the oscillations of a resource can control the two states, and can predict
848 breakdown of oscillation fairly well, as observed in experiments. From the very large set
849 of metabolites known to oscillate during the YMC (Tu *et al.*, 2007; Mohler *et al.*, 2008),
850 our model constrains possibilities to a few, that oscillate in a way that can permit such a
851 bistability to exist. From this, and consistent with extensive experimental data
852 (discussed earlier, and in Figure 5), it is possible to make parsimonious arguments for
853 acetyl-CoA (coincident with NADPH) as the metabolic resources controlling transitions
854 from quiescence to growth, and *vice versa*. Our model helps differentiate this small set
855 of metabolites from other metabolites that are important to maintain oscillations, but not
856 initiate them (i.e. they may only allow the cell to continue in one state, or the other). For
857 example, sulfur metabolism is critical to maintain oscillations (Murray *et al.*, 2003, 2007;
858 Tu *et al.*, 2007). It is also essential for the completion of a growth program, post entry
859 into the high oxygen consuming phase. But this metabolite peaks *after* acetyl-CoA in the
860 YMC (Tu *et al.*, 2007), and can be viewed as a consequence of initiating a growth

861 program, and also critical to sustain/complete this growth program, but not to initiate the
862 oscillation. Substantiating this explanation is the fact that sulfur metabolism is highly
863 dependent upon the utilization of NADPH for reduction, and NADPH (as described
864 earlier) is coincident with acetyl-CoA. A similar argument can be made for the
865 sustained, high respiration seen in the YMC, which produces ATP that will be required
866 to maintain the growth program once committed to by the cell. Separately, other studies
867 have shown that "quiescent" cells can show metabolic oscillations without entry into the
868 CDC (Slavov *et al.*, 2011). Here, these cells appear to show a commitment to the CDC
869 during these oscillations, based on gene expression patterns (Slavov *et al.*, 2011). This
870 can also be viewed through our interpretation of the commitment of cells to the CDC
871 due to a central resource. Cells will commit to the CDC, which however may not be
872 completed if a subsequent metabolic resource, normally dependent upon the
873 central/controlling resource (predicted to be acetyl-CoA/NADPH here), becomes
874 limiting. In other words, for a cell, usually if this committing resource is at the correct
875 threshold, other resources should not be limiting unless artificially constrained in an
876 experimental set-up. In (Slavov *et al.*, 2011), the limiting resource was phosphate, which
877 typically should be available and not limiting, and be assimilated into nucleotides in an
878 NADPH and acetyl-CoA dependent manner. If in a specific instance this resource
879 becomes limiting, the cells would commit to the growth/CDC state, but will not be able to
880 complete this, and will fall back into the Q state.
881
882 Our model provides a foundation to build new models to resolve other aspects observed
883 during the YMCs. First, in each cycle of the YMC, a fraction of the cells exit quiescence
884 and divide. It is not fully clear if the same cell divides in each cycle, or if a cell that has
885 entered division in one cycle does not in the next, and so on. The decision to divide has
886 been viewed as a stochastic, but irreversible step (Laxman *et al.*, 2010; Burnetti *et al.*,
887 2015). While our model as it stands cannot directly address these questions, the
888 dependence of the oscillations on the build-up and utilization of a specific resource,
889 allows the following argument to be made. First, the decision to divide in a cell would be
890 purely made by the amount of resource (acetyl-CoA) that has been built up in the cell.
891 Once acetyl-CoA reaches a certain threshold, the decision to divide is irreversible.

892 However, the build up of acetyl-CoA within an individual cell itself would be dependent
893 on small differences in overall metabolic homeostasis (compared to its neighbor), and
894 thus which cell reaches the threshold level first could be purely stochastic. Second, we
895 may speculate that if a cell has reached this threshold level and then used up its
896 resource during division, it is unlikely to be in a position to divide in the next round/next
897 cycle, whereas a cell that had not reached the threshold level in the previous cycle
898 would be best poised to divide instead. Our model does not take this into account, but it
899 provides a framework within which one could model the entire distribution of cells in
900 different Q/G states and with different levels of the resource. Despite the overall
901 stochastic aspect of Q-G transitions, such models would be able to make testable
902 predictions about the switching process even at the level of single cells. It is also
903 apparent that this level of synchrony requires high cell density in the system.
904 Separately, most studies have noted that upon initiating feeding in the chemostat, there
905 is a short period of tiny, non-robust oscillations. Based on our model, we would argue
906 that this is a situation where the quiescent cells are all now building up just sufficient
907 reserves of acetyl-CoA, within this stochastic process, and are starting to divide, but the
908 unusual steady-state condition in the chemostat will eventually lead to stable
909 oscillations.
910
911 Finally: Given the existing frameworks to describe Q-G state oscillations, our model is
912 necessarily coarse grained, and is intended only to build a more rigorous conceptual
913 framework within which to investigate the process of cells switching between
914 quiescence and growth states. For instance, it is straightforward to extend our models,
915 by adding space and diffusion processes, to account for scenarios where nutrients are
916 not well mixed and equally accessible, and where there is a high degree of spatial
917 rigidity within cell populations. It is also easy to alter other assumptions underlying our
918 model. For instance, our conclusions regarding acetyl-CoA being the driving resource
919 depend on an assumption we made in building the model that G cells consume the
920 resource. While this is biologically plausible, mathematically we could have assumed
921 the opposite, namely that the resource is consumed by cells in the Q state and not by
922 cells in the G state. In that case too our model could give similar oscillations - switching

923 rates would still need to be density/resource dependent, but the form of dependence on
924 resource would need to be reversed so that the high and low-q branches would be the
925 mirror images, with the low *q* branch being the only one at low *a* and the high *q* branch
926 being the only one at large values of *a*. And hence the waveform of the oscillating
927 resource would be flipped compared to Figures 2 and 3 - i.e., when *q* is high *a* would be
928 decreasing, while when *q* is low *a* would be increasing. If one could find a metabolite
929 that exhibited this waveform, then that metabolite would be an equally likely possibility
930 as a driver of the Q-G transition, except that it would have to act such that it caused a
931 switch from Q to G when it crossed a low threshold, or caused the opposite transition
932 when it crossed a high threshold. From the considerable data available, we have not
933 found a reasonable molecule with such a reversed waveform. Moreover, we know of no
934 process which consumes a metabolite in the Q state in the way described, so for now
935 acetyl-CoA driving the Q-G transition and being consumed during growth is the most
936 parsimonious explanation. Nevertheless, this shows how our framework could be easily
937 used in alternate scenarios.
938
939 Currently, existing experimental approaches to study such metabolically-driven Q-G
940 oscillations are very limited. Crude readouts, such as oxygen consumption, have very
941 limited resolution even to show the Q and G states, as the bistability begins to break
942 down. Gene expression analysis (even when done in single cells) is a late, end-point
943 readout which cannot explain this bistability but instead occurs after a switch. The key to
944 experimentally studying such bistability, therefore, will be the development of in vivo
945 intracellular metabolic sensors with excellent dynamic range and sensitivity, for
946 metabolites like acetyl-CoA or NADPH. This will allow the development of more precise
947 models to predict commitment steps, and identify differences within the population of
948 cells, that will help understand reversibility (between states), hysteresis and other
949 apparent phenomena.
950
951
952
953

954 **Methods**

955 *Experimental methods and data sets:*

956 Chemostat culture and cell division datasets: All dO2 data were obtained from YMCs
957 set up similar to already published data (Tu *et al.*, 2005, 2007; Kudlicki *et al.*, 2007;
958 Mohler *et al.*, 2008). In these studies, yeast cells were grown in chemostat cultures
959 using semi-defined medium, and yeast metabolic cycles were set up as described
960 earlier (Tu *et al.*, 2005; Tu, 2010). Data for cell division across three metabolic cycles
961 was obtained from earlier studies (Tu *et al.*, 2005; Laxman *et al.*, 2010). YMC gene
962 expression and metabolite datasets: Gene expression datasets were obtained from (Tu
963 *et al.*, 2005; Kudlicki *et al.*, 2007), and metabolite oscillation datasets were obtained
964 from (Tu *et al.*, 2007; Mohler *et al.*, 2008; Cai *et al.*, 2011; Machné and Murray, 2012),
965 including acetyl-CoA oscillation datasets.

966

967 *Parameter values and their q/a dependencies*

968

969 Figures 2C, 3C(i), 4A(ii), 4B(ii), 5A and 5B (default choices):

970 To produce the oscillation shown in these figures, we make the following choices (within
971 scenario 3c):

972 γ=1.665 hr^{-1}. σ=0.3996 hr^{-1}, μ=1, ν_{GQ}=16.65 hr^{-1}, $\nu_{QG}=h(q)$, where $h(q)$ is the Hill function
973 $h(q) = \nu_m(1+\beta(q/K)^{20})/(1+(q/K)^{20})$ with β=0.01, $K=a^2/(0.75^2+a^2)$, ν_m=16.65x(1.65-1.25K).
974 We use this Hill function with such a high Hill coefficient to approximate a step function
975 which drops rapidly from ν_m to $\beta\nu_m$ at $q=K$.

976

977 Figure 4, other panels:

978 The other panels of Fig 4 are made using exactly the same equations and parameter
979 choices as above, except for varying σ and γ as mentioned in the Fig 4 caption.

980

981 Figure 3C, other panels:

982 As above, except that

983 (ii) ν_m=16.65x(1.65-1.25K)x2.25K hr^{-1} and σ=0.3596 hr^{-1}.

984 (iii) ν_m=16.65x(1.65-1.25K)+16.65x1.85a^{10}/(200+a^{10}) hr^{-1} and σ=0.3297 hr^{-1}.

(iv) ν_m=16.65x2.25K hr^{-1} and σ=0.3397 hr^{-1}.

σ values were varied in order to keep the time period close to 4 hours.

Figure 5C, addition of bolus:

Until time t = 11.5 hours, the simulation is the same as in Fig 2C. At t = 11.5 hrs, the resource level is abruptly changed to 1.75 (just above its peak value in previous cycles, which was 1.73), and then the simulation is continued with the same equations and parameter values.

In all the above cases, the simulations were started, at t = 0 hours, with initial conditions q=1 and a=10^{-6} (i.e., we start with all cells in a quiescent state and starved of the resource). Simulations and figures were produced in Matlab. We used the ode45 differential equation integrator. The code is provided in Supplemental material. As extra controls, we checked that the stiff solver ode15s also provided the same results for the simulations in Fig 2 and 5, and a Mathematica notebook which repeats many of the same simulations, using the default NDSolve algorithm within Mathematica, is also provided with the Supplemental material.

Acknowledgements

SK is supported by funds from the Simons Foundation, and institutional support from NCBS-TIFR. SL is supported by a Wellcome Trust-DBT IA Intermediate Fellowship (IA/I/14/2/501523), and institutional support from inStem and the Department of Biotechnology.

1009 **References**

1010

1011 Ackermann, M. (2015). A functional perspective on phenotypic heterogeneity in
1012 microorganisms. Nat. Rev. Microbiol. *13*, 497–508.
1013 Angeli, D., Ferrell, J. E., and Sontag, E. (2004). Detection of multistability, bifurcations,
1014 and hysteresis in a large class of biological positive-feedback systems. Proc. Natl.
1015 Acad. Sci. *101*, 1822–1827.
1016 Avery, S. (2006). Microbial cell individuality and the underlying sources of
1017 heterogeneity. Nat. Rev. Microbiol. *4*, 577–587.
1018 Balthasar, van der P. (1926). “On Relaxation-Oscillations”. London, Edinburgh, Dublin
1019 Philos. Mag. *2*, 978–992.
1020 Brauer, M. J., Huttenhower, C., Airoldi, E. M., Rosenstein, R., Matese, J. C., Gresham,
1021 D., Boer, V. M., Troyanskaya, O. G., and Botstein, D. (2008). Coordination of Growth
1022 Rate, Cell Cycle, Stress Response, and Metabolic Activity in Yeast. Mol. Biol. Cell *19*,
1023 352–267.
1024 Burnetti, A. J., Aydin, M., and Buchler, N. E. (2015). Cell cycle Start is coupled to entry
1025 into the yeast metabolic cycle across diverse strains and growth rates. Mol. Biol. Cell
1026 *XXXIII*, 81–87.
1027 Cai, L., Sutter, B. M., Li, B., and Tu, B. P. (2011). Acetyl-CoA induces cell growth and
1028 proliferation by promoting the acetylation of histones at growth genes. Mol. Cell *42*,
1029 426–437.
1030 Cai, L., and Tu, B. P. (2012). Driving the Cell Cycle Through Metabolism. Annu. Rev.
1031 Cell Dev. Biol. *28*, 59–87.
1032 Cairns, R. A., Harris, I. S., and Mak, T. W. (2011). Regulation of cancer cell metabolism.
1033 Nat. Rev. Cancer *11*, 85–95.
1034 Campbell, K. *et al.* (2015). Self-establishing communities enable cooperative metabolite
1035 exchange in a eukaryote. Elife *4*, 1–23.
1036 Campbell, K., Vowinckel, J., and Ralser, M. (2016). Cell-to-cell heterogeneity emerges
1037 as consequence of metabolic cooperation in a synthetic yeast community. Biotechnol. J.
1038 *11*, 1169–1178.
1039 Chance, B., Estabrook, R., and Ghosh, A. (1964). DAMPED SINUSOIDAL

1040 OSCILLATIONS OF CYTOPLASMIC REDUCED PYRIDINE NUCLEOTIDE IN YEAST
1041 CELLS. Proc. Natl. Acad. Sci. U. S. A. *51*, 1244–1251.
1042 Chen, H., Fujita, M., Feng, Q., Clardy, J., and Fink, G. R. (2004). Tyrosol is a quorum-
1043 sensing molecule in Candida albicans. Proc. Natl. Acad. Sci. U. S. A. *101*, 5048 LP-
1044 5052.
1045 Coller, H. A., Sang, L., and Roberts, J. M. (2006). A New Description of Cellular
1046 Quiescence. PLoS Biol. *4*, e83.
1047 Conlon, I., and Raff, M. (2003). Differences in the way a mammalian cell and yeast cells
1048 coordinate cell growth and cell-cycle progression. J. Biol. *2*.
1049 Cooper, S. (1998). On the proposal of a G0 phase and the restriction point. FASEB J.
1050 *12*, 367–373.
1051 Cooper, S. (2003). Reappraisal of serum starvation, the restriction point, G0, and G1
1052 phase arrest points . FASEB J. *17*, 333–340.
1053 Cross, F., Archambault, V., Miller, M., and Klovstad, M. (2002). Testing a mathematical
1054 model of the yeast cell cycle. Mol. Biol. Cell *13*, 52–70.
1055 Daignan-Fornier, B., and Sagot, I. (2011). Proliferation/Quiescence: When to start?
1056 Where to stop? What to stock? Cell Div. *6*, 20.
1057 Daignan-Fornier B and Sagot I (2011). Proliferation / quiescence : the controversial “
1058 aller-retour .” Cell Div. *6*, 2–5.
1059 Dhawan, J., and Laxman, S. (2015). Decoding the stem cell quiescence cycle - lessons
1060 from yeast for regenerative biology. J. Cell Sci. *128*, 4467–4474.
1061 Farewell, A., Magnusson, L. U., and Nyström, T. (2005). ppGpp: a global regulator in
1062 Escherichia coli. Trends Microbiol. *13*, 236–242.
1063 Ferrell, J. E. (2011). Simple Rules for Complex Processes: New Lessons from the
1064 Budding Yeast Cell Cycle. Mol. Cell *43*, 497–500.
1065 Ferrell, J. E., Pomerening, J., Kim, S. Y., Trunnell, N. B., Xiong, W., Huang, C.-Y. F.,
1066 and Machleder, E. M. (2009). Simple, realistic models of complex biological processes:
1067 Positive feedback and bistability in a cell fate switch and a cell cycle oscillator. FEBS
1068 Lett. *583*, 3999–4005.
1069 Futcher, B. (2006). Metabolic cycle , cell cycle , and the finishing kick to Start.
1070 Goldbeter, A. (1991). A minimal cascade model for the mitotic oscillator involving cyclin

1071 and cdc2 kinase. Proc. Natl. Acad. Sci. *88*, 9107–9111.
1072 Goranov, A. I., Gulati, A., Dephoure, N., Takahara, T., Maeda, T., Gygi, S. P., Manalis,
1073 S., and Amon, A. (2013). Changes in cell morphology are coordinated with cell growth
1074 through the TORC1 pathway. Curr. Biol. *23*, 1269–1279.
1075 Gray, J. V, Petsko, G. a, Johnston, G. C., Ringe, D., Singer, R. a, and Werner-
1076 washburne, M. (2004). ' ' Sleeping Beauty ' ': Quiescence in Saccharomyces cerevisiae
1077 " Sleeping Beauty ": Quiescence in Saccharomyces cerevisiae †. Microbiol. Mol. Biol.
1078 Rev. *68*, 187–206.
1079 Han, Z., Yang, L., MacLellan, R. W., Weiss, J. N., and Qu, Z. (2005). Hysteresis and
1080 Cell Cycle Transitions: How Crucial Is It? Biophys. J. *88*, 1626–1634.
1081 Hartwell, L. H. (1974). Saccharomyces cerevisiae cell cycle. Bacteriol. Rev. *38*, 164–
1082 198.
1083 Heiden, M. G. Vander, Cantley, L. C., Thompson, C. B., Vander Heiden, M. G., Cantley,
1084 L. C., and Thompson, C. B. (2009). Understanding the Warburg Effect: The Metabolic
1085 Requirements of Cell Proliferation. Science (80-.). *324*, 1029–1033.
1086 Hess, B., and Boiteux, A. (1971). Oscillatory Phenomena in Biochemistry. Annu. Rev.
1087 Biochem. *40*, 237–258.
1088 Holland, S. L., Reader, T., Dyer, P. S., and Avery, S. V. (2014). Phenotypic
1089 heterogeneity is a selected trait in natural yeast populations subject to environmental
1090 stress. Environ. Microbiol. *16*, 1729–1740.
1091 Hommes, F. (1964). OSCILLATORY REDUCTIONS OF PYRIDINE NUCLEOTIDES
1092 DURING ANAEROBIC GLYCOLYSIS IN BREWERS' YEAST. Arch. Biochem. Biophys.
1093 *108*, 36–46.
1094 Ibanez, A. J., Fagerer, S. R., Schmidt, A. M., Urban, P. L., Jefimovs, K., Geiger, P.,
1095 Dechant, R., Heinemann, M., and Zenobi, R. (2013). Mass spectrometry-based
1096 metabolomics of single yeast cells. Proc. Natl. Acad. Sci. *110*, 8790–8794.
1097 J, T. J. (1991). Modeling the cell division cycle: cdc2 and cyclin interactions. Proc. Natl.
1098 Acad. Sci. *88*, 7328–7332.
1099 Johnston, G. C., Pringle, J. R., and Hartwell, L. H. (1977). Coordination of growth with
1100 cell division in the yeast Saccharomyces cerevisiae. Exp. Cell Res. *105*, 79–98.
1101 Jorgensen, P., Rupeš, I., Sharom, J. R., Schneper, L., Broach, J. R., and Tyers, M.

1102 (2004). A dynamic transcriptional network communicates growth potential to ribosome
1103 synthesis and critical cell size. Genes Dev. *18*, 2491–2505.
1104 Jules, M., François, J., and Parrou, J. L. (2005). Autonomous oscillations in
1105 Saccharomyces cerevisiae during batch cultures on trehalose. FEBS J. *272*, 1490–
1106 1500.
1107 Kalucka, J. *et al.* (2015). Metabolic control of the cell cycle. Cell Cycle *4101*, 3379–
1108 3388.
1109 Kaplon, J., Dam, L. Van, Peeper, D., Kaplon, J., Dam, L. Van, and Peeper, D. (2015).
1110 Two-way communication between the metabolic and cell cycle machineries : the
1111 molecular basis. Cell Cycle *14*, 2022–2032.
1112 Keulers, M., Suzuki, T., Satroutdinov, A., and Kuriyama, H. (1996). Autonomous
1113 metabolic oscillation in continuous culture of Saccharomyces cerevisiae grown on
1114 ethanol. FEMS Microbiol. Lett. *142*, 253–258.
1115 Klevecz, R. R., Bolen, J., Forrest, G., and Murray, D. B. (2004). A genomewide
1116 oscillation in transcription gates DNA replication and cell cycle. Proc. Natl. Acad. Sci.
1117 *101*, 1200–1205.
1118 Klosinska, M. M., Crutchfield, C. A., Bradley, P. H., Rabinowitz, J. D., and Broach, J. R.
1119 (2011). Yeast cells can access distinct quiescent states. Genes Dev. *25*, 336–349.
1120 Krishna, S., Semsey, S., and Jensen, M. (2009). Frustrated bistability as a means to
1121 engineer oscillations in biological systems. Phys. Biol. *6*, 036009.
1122 Kudlicki, A., Rowicka, M., and Otwinowski, Z. (2007). SCEPTRANS: an online tool for
1123 analyzing periodic transcription in yeast . Bioinformatics *23*, 1559–1561.
1124 Küenzi, M. T., and Fiechter, A. (1969). Changes in carbohydrate composition and
1125 trehalase-activity during the budding cycle of Saccharomyces cerevisiae. Arch.
1126 Mikrobiol. *64*, 396–407.
1127 Laporte, D., Lebaudy, A., Sahin, A., Pinson, B., Ceschin, J., Daignan-Fornier, B., and
1128 Sagot, I. (2011). Metabolic status rather than cell cycle signals control quiescence entry
1129 and exit. J. Cell Biol. *192*, 949–957.
1130 Laxman, S., Sutter, B. M., and Tu, B. P. (2010). Behavior of a metabolic cycling
1131 population at the single cell level as visualized by fluorescent gene expression
1132 reporters. PLoS One *5*, e12595.

1133 Lee, I. H., and Finkel, T. (2013). Metabolic regulation of the cell cycle. Curr. Opin. Cell
1134 Biol. *25*, 724–729.
1135 Lewis, D., and Gattie, D. (1991). The Ecology of Quiescent Microbes. U.S. Environ.
1136 Prot. Agency, Washington, D.C. *EPA/600/J-*.
1137 Lloyd, D., and Murray, D. B. (2005). Ultradian metronome: timekeeper for orchestration
1138 of cellular coherence. Trends Biochem. Sci. *30*, 373–377.
1139 Machné, R., and Murray, D. B. (2012). The yin and yang of yeast transcription:
1140 elements of a global feedback system between metabolism and chromatin. PLoS One
1141 *7*, e37906.
1142 Mellor, J. (2016). The molecular basis of metabolic cycles and their relationship to
1143 circadian rhythms. Nat. Struct. Mol. Biol. *23*, 1035–1044.
1144 Miller, M. B., and Bassler, B. L. (2001). Quorum Sensing in Bacteria. Annu. Rev.
1145 Microbiol. *55*, 165–199.
1146 Mirchenko, L., and Uhlmann, F. (2010). Sli15(INCENP) dephosphorylation prevents
1147 mitotic checkpoint reengagement due to loss of tension at anaphase onset. Curr. Biol.
1148 *20*, 1396–1401.
1149 Mohler, R., Tu, B. P., Dombek, K. M., Hoggard, J., Young, E., and Synovec, R. E.
1150 (2008). Identification and evaluation of cycling yeast metabolites in two-dimensional
1151 comprehensive gas chromatography-time-of-flight-mass spectrometry data. J.
1152 Chromatogr. A *1186*, 401–411.
1153 Murray, D. B., Beckmann, M., and Kitano, H. (2007). Regulation of yeast oscillatory
1154 dynamics. Proc. Natl. Acad. Sci. U. S. A. *194*, 2241–2246.
1155 Murray, D. B., Klevecz, R., and Lloyd, D. (2003). Generation and maintenance of
1156 synchrony in Saccharomyces cerevisiae continuous culture. Exp. Cell Res. *287*, 10–15.
1157 Nelson, DL; Cox, M. (2017). Principles of biochemistry, NY, USA: W. H. Freeman.
1158 Norel, R., and Agur, Z. (1991). A model for the adjustment of the mitotic clock by cyclin
1159 and MPF levels. Science (80-.). *251*, 1076–1078.
1160 Novak, B., and Tyson, J. J. (1993). Numerical analysis of a comprehensive model of M-
1161 phase control in Xenopus oocyte extracts and intact embryos. J. Cell Sci. *106*, 1153–
1162 1168.
1163 Novák, B., and Tyson, J. J. (2008). Design principles of biochemical oscillators. Nat.

1164 Rev. Mol. Cell Biol. *9*, 981–991.
1165 Patra, K. C., and Hay, N. (2014). The pentose phosphate pathway and cancer. Trends
1166 Biochem. Sci. *39*, 347–354.
1167 Pigolotti, S., Krishna, S., and Jensen, M. H. (2007). Oscillation patterns in negative
1168 feedback loops. Proc. Natl. Acad. Sci. *104*, 6533 LP-6537.
1169 Pomerantz, S. C., and McCloskey, J. A. (1990). Analysis of RNA Hydrolyzates by Liquid
1170 Chromatography-Mass Spectrometry. Methods Enzymol. *193*, 796–824.
1171 Pomerening, J., Sontag, E., and Ferrell, J. E. (2003). Building a cell cycle oscillator:
1172 hysteresis and bistability in the activation of Cdc2. Nat. Cell Biol. *5*, 346–351.
1173 Robertson, J. B., Stowers, C. C., Boczko, E., and Johnson, C. H. (2008). Real-time
1174 luminescence monitoring of cell-cycle and respiratory oscillations in yeast. Proc. Natl.
1175 Acad. Sci. U. S. A. *105*, 17988–17993.
1176 Rowicka, M., Kudlicki, A., Tu, B. P., and Otwinowski, Z. (2007). High-resolution timing of
1177 cell cycle-regulated gene expression. Proc. Natl. Acad. Sci. U. S. A. *104*, 16892–16897.
1178 Satroutdinov, A. D., Kuriyama, H., and Kobayashi, H. (1992). Oscillatory metabolism of
1179 Saccharomyces cerevisiae in continuous culture. FEMS Microbiol. Lett. *77*, 261–267.
1180 Schauder, S., Shokat, K., Surette, M. G., and Bassler, B. L. (2001). The LuxS family of
1181 bacterial autoinducers: biosynthesis of a novel quorum-sensing signal molecule. Mol.
1182 Microbiol. *41*, 463–476.
1183 Shan, C. *et al.* (2014). Lysine acetylation activates 6-phosphogluconate dehydrogenase
1184 to promote tumor growth. Mol. Cell *55*, 552–565.
1185 Shi, L., Sutter, B. M., Ye, X., and Tu, B. P. (2010). Trehalose is a key determinant of the
1186 quiescent metabolic state that fuels cell cycle progression upon return to growth. Mol.
1187 Biol. Cell *21*, 1982–1990.
1188 Shi, L., and Tu, B. P. (2013). Acetyl-CoA induces transcription of the key G1 cyclin
1189 CLN3 to promote entry into the cell division cycle in Saccharomyces cerevisiae. Proc.
1190 Natl. Acad. Sci. *110*, 7318–7323.
1191 Shi, L., and Tu, B. P. (2014). Protein acetylation as a means to regulate protein function
1192 in tune with metabolic state. Biochem. Soc. Trans. *42*, 1037–1042.
1193 Silverman, S. J. *et al.* (2010). Metabolic cycling in single yeast cells from
1194 unsynchronized steady-state populations limited on glucose or phosphate. Proc. Natl.

1195 Acad. Sci. U. S. A. *107*, 6946–6951.
1196 Slavov, N., and Botstein, D. (2011). Coupling among growth rate response, metabolic
1197 cycle, and cell division cycle in yeast. Mol. Biol. Cell *22*, 1997–2009.
1198 Slavov, N., and Botstein, D. (2013). Decoupling nutrient signaling from growth rate
1199 causes aerobic glycolysis and deregulation of cell size and gene expression. Mol. Biol.
1200 Cell *24*, 157–168.
1201 Slavov, N., Macinskas, J., Caudy, A., and Botstein, D. (2011). Metabolic cycling without
1202 cell division cycling in respiring yeast. Proc. Natl. Acad. Sci. U. S. A. *108*, 19090–19095.
1203 Solomon, M. J. (2003). Hysteresis meets the cell cycle. Proc. Natl. Acad. Sci. *100*, 771–
1204 772.
1205 Srivatsan, A., and Wang, J. D. (2008). Control of bacterial transcription, translation and
1206 replication by (p)ppGpp. Curr. Opin. Microbiol. *11*, 100–105.
1207 Strogatz, S. (1994). Nonlinear Dynamics and Chaos., Reading, MA: Addison-Wesley.
1208 Sumner, E. R., and Avery, S. V (2017). Phenotypic heterogeneity : differential stress
1209 resistance among individual cells of the yeast Saccharomyces cerevisiae. Microbiology
1210 *1941*, 14–345.
1211 Tiana, G., Krishna, S., Pigolotti, S., Jensen, M., and Sneppen, K. (2007). Oscillations
1212 and temporal signalling in cells. Phys. Biol. *4*, R1-17.
1213 Tsai, T., Choi, Y., Ma, W., Pomerening, J., Tang, C., and Ferrell, J. E. (2008). Robust,
1214 tunable biological oscillations from interlinked positive and negative feedback loops.
1215 Science (80-.). *321*, 126–129.
1216 Tu, B. P. (2010). Ultradian metabolic cycles in yeast. Methods Enzymol. *470*, 857–866.
1217 Tu, B. P., Kudlicki, A., Rowicka, M., and McKnight, S. L. (2005). Logic of the yeast
1218 metabolic cycle: temporal compartmentalization of cellular processes. Science *310*,
1219 1152–1158.
1220 Tu, B. P., Mohler, R. E., Liu, J. C., Dombek, K. M., Young, E. T., Synovec, R. E., and
1221 McKnight, S. L. (2007). Cyclic changes in metabolic state during the life of a yeast cell.
1222 Proc. Natl. Acad. Sci. U. S. A. *104*, 16886–16891.
1223 Tyson, J. J., Chen, K. C., and Novak, B. (2003). Sniffers, buzzers, toggles and blinkers:
1224 Dynamics of regulatory and signaling pathways in the cell. Curr. Opin. Cell Biol. *15*,
1225 221–231.

1226 Tyson, J. J., and Novak, B. (2001). Regulation of the Eukaryotic Cell Cycle: Molecular
1227 Antagonism, Hysteresis, and Irreversible Transitions. J. Theor. Biol. *210*, 249–263.
1228 Tyson, J. J., and Novák, B. (2015). Models in biology: lessons from modeling regulation
1229 of the eukaryotic cell cycle. BMC Biol. *13*, 46.
1230 Veening, J., Igoshin, O., Eijlander, R., Nijland, R., Hamoen, L., and OP, K. (2008).
1231 Transient heterogeneity in extracellular protease production by Bacillus subtilis. Mol.
1232 Syst. Biol. *4*.
1233 De Virgilio, C. (2012). The essence of yeast quiescence. FEMS Microbiol. Rev. *36*,
1234 306–339.
1235 Wei, S., Moore, J., Chen, K., Lassaletta, A. D., Yi, C.-S., Tyson, J. J., and Sible, J. C.
1236 (2003). Hysteresis drives cell-cycle transitions in Xenopus laevis egg extracts. Proc.
1237 Natl. Acad. Sci. *100*, 975–980.
1238 Whitehead, N. A., Barnard, A. M. L., Slater, H., Simpson, N. J. L., and Salmond, G. P.
1239 C. (2001). Quorum-sensing in Gram-negative bacteria. FEMS Microbiol. Rev. *25*, 365–
1240 404.
1241 Yao, G., Tan, C., West, M., Nevins, J. R., and You, L. (2011). Origin of bistability
1242 underlying mammalian cell cycle entry. Mol. Syst. Biol. *7*, 485.
1243 Zhu, J., Chai, Y., Zhong, Z., Li, S., and Winans, S. C. (2003). Agrobacterium Bioassay
1244 Strain for Ultrasensitive Detection of N-Acylhomoserine Lactone-Type Quorum-Sensing
1245 Molecules: Detection of Autoinducers in Mesorhizobium huakuii. Appl. Environ.
1246 Microbiol. *69*, 6949–6953.
1247